1521-009X/42/1/44–61$25.00
DRUG METABOLISM AND DISPOSITION

http://dx.doi.org/10.1124/dmd.113.052670
Drug Metab Dispos 42:44–61, January 2014

DRUG METABOLISM & DISPOSITION

MicroRNA-561 Promotes Acetaminophen-Induced Hepatotoxicity in HepG2 Cells and Primary Human Hepatocytes through Downregulation of the Nuclear Receptor Corepressor Dosage-Sensitive Sex-Reversal Adrenal Hypoplasia Congenital Critical Region on the X Chromosome, Gene 1 (DAX-1)[S]

Minghua Li, Yinxue Yang, Zhi-Xu He, Zhi-Wei Zhou, Tianxin Yang, Peixuan Guo, Xueji Zhang, and Shu-Feng Zhou

Department of Pharmaceutical Sciences, College of Pharmacy, University of South Florida, Tampa, Florida (M.L., Z.W.Z., S.F.Z.); Department of Hepatobiliary Surgery, General Hospital of Ningxia Medical University, Yinchuan City, Ningxia Hui Autonomous Region, China (Y.Y.); Guizhou Provincial Key Laboratory for Regenerative Medicine, Stem Cell and Tissue Engineering Research Center, Guiyang Medical University, Guiyang, Guizhou, China (Z.X.H.); Department of Internal Medicine, University of Utah and Salt Lake Veterans Affairs Medical Center, Salt Lake City, Utah (T.Y.); Nanobiotechnology Center and Markey Cancer Center, College of Pharmacy, University of Kentucky, Lexington, Kentucky (P.G.); Research Center for Bioengineering and Sensing Technology, University of Science and Technology Beijing, Beijing, China (X.Z.)

Received May 8, 2013; accepted October 8, 2013

ABSTRACT

One of the major mechanisms involved in acetaminophen (APAP)-induced hepatotoxicity is hepatocyte nuclear factor 4α (HNF4α)-mediated activation of pregnane X receptor (PXR) and constitutive androstane receptor (CAR). In the present study, we investigated the role of miR-561 and its target gene *DAX-1* encoding a corepressor of HNF4α in the process of APAP-induced hepatotoxicity. We used both human hepatocellular liver carcinoma cell line (HepG2) cells and primary human hepatocytes in this study and monitored the levels of reactive oxygen species, lactate dehydrogenase, and glutathione. Our bioinformatics study suggests an association between miR-561 and DAX-1, but not HNF4α. Treatment of HepG2 cells with APAP significantly reduced the expression of DAX-1 in a concentration-dependent manner. miR-561 was induced by APAP treatment in HepG2 cells. Transfection of HepG2 cells with an miR-561 mimic exacerbated APAP-induced hepatotoxicity. HNF4α is physically associated with DAX-1 in HepG2 cells. A decreased protein level of DAX-1 by APAP treatment was also enhanced by miR-561 mimic transfection in HepG2 cells and primary human hepatocytes. The basal and APAP-induced expression of PXR and CAR was enhanced by miR-561 mimic transfection; however, transfection of HepG2 cells or primary human hepatocytes with a miR-561 inhibitor or DAX-1 small interfering RNA reversed these effects. Additionally, the chromatin immunoprecipitation assay revealed that recruitment of DAX-1 onto the *PXR* promoter was inversely correlated with the recruitment of peroxisome proliferator–activated receptor-α coactivator-1α and HNF4α on APAP treatment. These results indicate that miR-561 worsens APAP-induced hepatotoxicity via inhibition of DAX-1 and consequent transactivation of nuclear receptors.

Introduction

Acetaminophen (APAP, *N*-acetyl-*p*-aminophenol, also known as paracetamol) is the most widely used analgesic and antipyretic agent. Nonetheless, intake of APAP over the recommended safe dose of 4 g per day can lead to severe liver damage and even liver failure in humans (Hinson et al., 2010). APAP overdose is the leading cause of acute liver failure in the United States and in most of Europe. With recommended dosage, APAP is considered a safe therapeutic agent and

The authors thank the Startup Fund of the College of Pharmacy, University of South Florida, Tampa, Florida, for financial support. Drs. Minghua Li and Zhi-Wei Zhou are holders of postdoctoral scholarships from the College of Pharmacy, University of South Florida, Tampa, Florida.

dx.doi.org/10.1124/dmd.113.052670.

[S]This article has supplemental material available at dmd.aspetjournals.org.

ABBREVIATIONS: ANOVA, analysis of variance; APAP, acetaminophen; CAR, constitutive androstane receptor; ChIP, chromatin immunoprecipitation assay; COUP, chicken ovalbumin upstream promoter; DAX-1, dosage-sensitive sex reversal adrenal hypoplasia congenital critical region on X chromosome, gene 1; DCFDA, 2′,7′-dichlorofluorescein diacetate; FXR, farnesoid X receptor; GAPDH, glyceraldehyde-3-phosphate dehydrogenase; GSH, glutathione; GW4064, 3-(2,6-dichlorophenyl)-4-(3′-carboxy-2-chlorostilben-4-yl)oxymethyl-5-isopropylisoxazole; HEPG2, human hepatocellular liver carcinoma cell line; HNF4α, hepatocyte nuclear factor 4α; IP, immunoprecipitation; LDH, lactate dehydrogenase; LXRα, liver X receptor-α; miRNA, microRNA; NAC, *N*-acetyl-L-cysteine; NAPQI, *N*-acetyl-*p*-benzoquinone; NR, nuclear receptor; PCR, polymerase chain reaction; PGC1α, peroxisome proliferator-activated receptor-α coactivator-1α; PVDF, polyvinylidene difluoride; PXR, pregnane X receptor; RIPA, radioimmunoprecipitation; ROS, reactive oxygen species; RT, reverse transcription; siRNA, small interfering RNA; SULT, sulfotransferase; UTR, untranslated region; WST-1, water-soluble 2-(4-iodophenyl)-3-(4-nitrophenyl)-5-(2,4-disulfophenyl)-2H-tetrazolium salt.

is rapidly metabolized to nontoxic compounds in the liver by phase II detoxifying enzymes, including uridine diphosphate-glucuronosyltransferases (UGTs) and sulfotransferases (SULTs) (Ronchetti et al., 2008). However, these phase II detoxification pathways will be saturated and alternative metabolic pathways by phase I cytochrome P450s will be greatly activated in the event of APAP overdose. APAP is metabolized by CYP1A2, 2D6, 2E1, and 3A4 to a highly reactive intermediate metabolite, *N*-acetyl-*p*-benzoquinone (NAPQI), with CYP3A4 being the major cytochrome catalyzing APAP oxidation to form NAPQI in human liver (see Supplemental Fig. 1) (Laine et al., 2009). NAPQI depletes glutathione (GSH) and subsequently causes covalent binding to important cellular proteins, initiates the formation of reactive oxygen species (ROS), promotes the release of proinflammatory cytokines such as tumor necrosis factor-α, and ultimately results in apoptosis and necrosis of hepatocytes (Tujios and Fontana, 2011; Zhao and Pickering, 2011). At subtoxic doses, NAPQI is inactivated by GSH conjugation, resulting in APAP cysteine and mercapturate conjugates (Laine et al., 2009).

The ligand-activated nuclear receptors (NRs) pregnane X receptor (PXR) and constitutive androstane receptor (CAR) are considered critical mediators that stimulate the transcriptional activation of a panel of their target genes such as *CYP3A4, CYP2B6, CYP2E1, SULT2A1,* and *MDR1/ABCB1* when hepatocytes are exposed to xenobiotics (Chai et al., 2013). In vitro studies have shown that the orphan nuclear receptor hepatocyte nuclear factor-4α (HNF4α) binds as a homodimer to the *cis*-acting element containing a direct repeat (DR1) sequence located within the distal xenobiotic responsive module of the *CYP3A4* gene, immediately upstream of *PXR/CAR* response elements. Furthermore, conditional deletion of *Hnf4α* in fetal mice led to reduced or absent expression *Cyp3a*, and conditional hepatic deletion of *Hnf4α* in adult mice also resulted in reduced basal and inducible expression of *Cyp3a* (Tirona et al., 2003). These results indicate that HNF4α determines PXR- and CAR-mediated xenobiotic induction of CYP3A4 in hepatocytes.

HNF4α is classified as an orphan nuclear receptor in humans and is expressed at high levels in the liver. Hepatic HNF4α-mediated regulation of its target genes is activated by elevation of cellular activity of its coactivator, peroxisome proliferator-activated receptor-γ coactivator-1α (PGC1α), a protein that is encoded by human *PPARGC1A* gene. Overexpression of the HNF4α corepressor, dosage-sensitive sex-reversal adrenal hypoplasia congenital critical region on X chromosome, gene 1 (DAX-1/NR0B1; for its gene structure, see Supplemental Fig. 2), decreased HNF4α-mediated target gene expression (Nedumaran et al., 2009). DAX-1 is well known to have a key role in steroidogenesis, adrenogonadal development, and maintenance of stem cell pluripotency (McCabe, 2007). Although DAX-1 is expressed at a low level in the liver, it plays an important role in repressing diverse nuclear receptors such as HNF4α, CAR, liver X receptor-α (LXRα), and farnesoid X receptor (FXR) (Nedumaran et al., 2009, 2010; Li et al., 2011; Laurenzana et al., 2012). DAX-1 appears to have a further role in hepatic lipogenesis and gluconeogenesis. DAX-1 can compete with NR coactivators such as PGC1α, glutamate receptor-interacting protein 1, and steroid receptor coactivator-1, and it recruits corepressors such as nuclear receptor corepressor 1 and Alien (Ehrlund and Treuter, 2012). The revealed crystal structure of DAX-1 bound to liver receptor homolog 1 has shown that DAX-1 could function as a ligand-independent NR as well as a competitive transcriptional corepressor (Fannin et al., 2010).

MicroRNA (miRNA) is a small noncoding RNA molecule (normally 20–24 nucleotides) that binds to the 3′-untranslated region (UTR) of target mRNAs and negatively regulates gene expression by blocking protein translation or by degrading the mRNA (Bartel, 2009). A mature miRNA is incorporated into a RNA-induced silencing complex, which recognizes target mRNAs through imperfect base pairing with the target miRNA. Increasing evidence suggests that aberrant expression of miRNAs such as miR-122 and miR-192 is involved in APAP-induced hepatotoxicity in humans and rodents (Jetten et al., 2012; Ward et al., 2012). Thus, miRNAs might be an attractive therapeutic target for APAP-caused hepatic injury. However, the specific miRNAs that are involved in APAP-induced hepatotoxicity remain unknown. This study investigated the role of DAX-1 in miR-561-mediated APAP-induced hepatotoxicity in human hepatocellular liver carcinoma cell line (HepG2) cells and primary human hepatocytes.

Materials and Methods

Bioinformatics Studies. Before starting the benchwork, we conducted a bioinformatics study to predict the miRNAs that could regulate human *DAX-1* and *HNF4α* genes and what targets were regulated by miR-561. Several algorithms were applied to predict the miRNAs that could regulate human *DAX-1* and *HNF4α* genes and the gene targets probably regulated by miR-561: TargetScan (http://www.targetscan.org/), miRDB (http://mirdb.org/miRDB/), and MicroCosm (http://www.ebi.ac.uk/enright-srv/microcosm). Human *miR-561* gene has been mapped to 2q32.1. The mature sequences of miR-561 are miR-561-3p and miR-561-5p (see Supplemental Fig. 3). miRanda (http://www.microrna.org/microrna/) was used to predict the targets of miR-561. TargetScan can predict the biologic targets of miRNAs by searching for the presence of conserved 8-mer and 7-mer sites matching the seed region of each miRNA (Lewis et al., 2005), with nonconserved sites predicted as well. In mammals, the prediction is ranked based on the predicted efficacy of targeting as calculated using the context + scores of the sites (Garcia et al., 2011). miRBD, a web-based database and tool, can predict miRNAs and their targets (Wang, 2008). All the targets are predicted by a bioinformatics tool MirTarget2, which has been developed by analyzing thousands of genes impacted by miRNAs with an SVM (Support Vector) learning machine. Common features associated with miRNA target binding have been identified and used to predict miRNAs' targets. miRanda can predict the target of miRNAs based on current biologic knowledge on target rules and on the use of an up-to-date compendium of mammalian microRNAs (Betel et al., 2008). Using an improved graphical interface, a user can explore: 1) the set of genes that are potentially regulated by a particular miRNA; 2) the implied cooperativity of multiple miRNAs on a particular mRNA; and 3) miRNA expression profiles in various tissues. This algorithm provides users with functional information about the growing number of miRNAs and their interaction with target genes in many species and facilitates novel discoveries in miRNA gene regulation. In addition, MicroCosm was used to predict the miRNAs that might regulate human *DAX-1* gene.

Chemicals and Reagents. APAP was obtained from Sigma-Aldrich Chemical Co. (St. Louis, MO). All other chemicals used were of the highest pure-grade available.

Cell Line and Cell Cultures. The human hepatocellular carcinoma cell line HepG2 was obtained from the American Type Culture Collection (Manassas, VA) and maintained in the logarithmic phase of growth in Dulbecco's modified Eagle's medium supplemented with heat-inactivated 10% fetal bovine serum (Invitrogen Life Technologies Co., Carlsbad, CA) and 2 mM L-glutamine (Sigma-Aldrich Chemical Co.) at 37°C in a 5% CO_2-95% air humidified incubator. Cryopreserved primary human hepatocytes were obtained from Invitrogen Life Technologies Co., and the cells were recovered and cultured according to following the manufacturer's protocol. The sex status of the donors was not clearly documented.

Cell Viability Assay. Cell viability was determined by the water-soluble 2-(4-iodophenyl)-3-(4-nitrophenyl)-5-(2,4-disulfophenyl)-2H-tetrazolium salt (WST-1) assay using a commercially available kit (Clontech Inc., Palo Alto, CA) according to the manufacturer's protocol. The assay is based on the cleavage of the tetrazolium salt WST-1 to formazan by cellular mitochondrial dehydrogenases. In brief, HepG2 cells were seeded at an initial density of 1×10^4 cells/well in 96-well plates and cultured at 37°C overnight. The cells were treated with various concentrations (0, 0.5, 1, 5, 10, 25, and 50 mM) of APAP for 24 hours and were then exposed to 5 μl of the WST-1 reagent for 1 hour at

37°C. Absorbance was measured using a Synergy H4 Hybrid microplate reader (BioTek Inc., Winooski, VT) at a wavelength of 450 nm. The concentration required for IC_{50} was determined from concentration-response curves (i.e., cell survival fraction vs. APAP concentration) obtained in multireplicated experiments by nonlinear regression analysis using the GraphPad Prism 6 software (San Diego, CA). The viability of untreated cells was considered 100%. Each experiment was carried out at least three times, and results are expressed as the mean ± S.D. for each determination.

Overexpression and Knockdown of miR-561 via Transfection. The nontargeting miRNA control, miR-561 mimic, and miR-561 inhibitor were obtained from Invitrogen Life Technologies Co. Human HepG2 cells were seeded in six-well plates at 2.5×10^5 cells/well and cultured for 18 hours and then transfected with 100 pmol miR-561 mimic, miR-561 inhibitor, or nontargeting control using Lipofectamine 2000 (Invitrogen Life Technologies Co.) according to the manufacturer's protocol. The specificity of miR-561 mimic and inhibitor was checked after transfection of HepG2 cells for 48 hours.

Luciferase Reporter Assay. HepG2 cells in 96-well plates were cotransfected with 100 ng of DAX-1-3′-UTR-luciferase reporter vectors (pLightSwitch_3′-UTR; SwitchGear Genomics Inc., Menlo Park, CA) and either 20 nM miR-561 mimic or 10 nM miR-561 inhibitor. β-Galactosidase (20-ng) vectors were used as an internal control for normalizing the transfection efficiency. All transfections were performed for 48 hours using the Lipofectamine 2000 (Invitrogen Life Technologies Co.) transfection reagent according to the manufacturer's instructions. Cell lysates were assayed for luciferase activity using the LightSwitch luciferase assay system (SwitchGear Genomics Inc., Menlo Park, CA).

Real-Time Polymerase Chain Reaction. The HepG2 cells were treated with APAP for 24 hours before harvesting and analysis. Total RNA was prepared using the Trizol reagent (Invitrogen Life Technologies Co.), and reverse transcription (RT) of total RNA to single-stranded cDNA was performed using oligo (dT) primer and the iScript reverse transcriptase supplied with the iScript cDNA Synthesis Kit (Bio-Rad Laboratories, Hercules, CA). Quantitative real-time polymerase chain reaction (PCR) amplification was performed using a LightCycler thermal cycler system with the use of FastStart Universal Probe Master (Roche Diagnostics Co., Indianapolis, IN). Gene-specific probe sets for human *PXR*, *CAR*, *HNF4α*, *DAX-1*, *PGC1α*, and glyceraldehyde-3-phosphate dehydrogenase (*GAPDH*) genes were purchased from Integrated DNA Technologies Inc. (Coralville, IA) (Table 1). The relative amount of target mRNA was calculated by the comparative cycle threshold method with *GAPDH* as the internal reference and expressed as the percentage change relative to empty vector transfected or untransfected controls. Quantification data were corrected for reaction efficiencies.

For miRNA analysis, total RNA was reverse-transcribed using the miScript RT kit (Qiagen Inc., Valencia, CA) according to the manufacturer's protocol. Polyadenylated miRNAs were converted to cDNAs using oligo(dT) and random primers containing a unique tag sequence at the 5′-end. Quantification of miRNAs was performed using the miScript SYBR Green PCR kit (Qiagen Inc.), and miRNA-specific 5′-primers for detection of miR-4666b, miR-4477, miR-3658, and miR-561 were purchased from Qiagen Inc. (Table 2). Internal control of miRNA analysis used the U6 small nuclear RNA purchased from Qiagen Inc. (Hs_RNU6-2_1 miScript Primer Assay, catalog no. MS00033740).

Coimmunoprecipitation Assay. The coimmunoprecipitation assay is often used to identify physiologically relevant protein-protein interactions using target protein-specific antibodies to indirectly capture proteins that are bound to a specific target protein. To investigate whether HNF4α was physically associated with DAX-1, we conducted the coimmunoprecipitation assay using HepG2 cells treated with APAP at 0.5, 1, or 5 mM for 24 hours. Briefly, HepG2 cells were harvested and lysed using the radioimmunoprecipitation assay (RIPA) lysis buffer (catalog no. sc-24948; Santa Cruz Biotechnology Inc., Santa Cruz, CA) freshly supplemented with phosphatase and protease inhibitors. Whole-cell lysates were precleared after adding the control IgG and 25% (v/v) protein A/G-agarose conjugate. The mixture was incubated for 30 minutes at 4°C and centrifuged at 1000*g* for 30 seconds at 4°C to precipitate the pellet; the supernatants (cell lysates) were collected to a new microcentrifuge tube at 4°C; 100 μg of precleared cellular lysates was incubated with the rabbit primary antibody against human HNF4α or DAX-1 (Santa Cruz Biotechnology Inc.) at 4°C overnight. The primary antibody-bound target protein complexed with its interacting protein was captured by protein A/G-agarose suspension (catalog no. sc-2003; Santa Cruz Biotechnology Inc.) after incubation at 4°C overnight. The pellet was collected after centrifugation at 1000*g* for 30 seconds and washed with RIPA buffer, and the aforementioned steps were repeated four times. After final wash, the supernatant was discarded and the pellet was resuspended in 2× electrophoresis sample buffer. The eluted protein complex was subjected to Western blotting analysis using the rabbit primary antibody against either HNF4α or DAX-1 (Santa Cruz Biotechnology Inc.). β-Actin was used as the internal control.

Determination of Cellular Lactate Dehydrogenase Content. Cellular lactate dehydrogenase (LDH) contents were determined by using a commercially available kit (catalog no. ab65393; Abcam Inc., Cambridge, MA,) according to the manufacturer's protocol. Briefly, HepG2 cells were cultured in a 96-well microplate at density of 1×10^4 cells/well. After transfection with a miR-561 mimic or inhibitor for 48 hours with or without APAP treatment for 24 hours, the culture medium was collected and centrifuged at 1500*g* for 10 minutes. An equal amount of the reaction mixture containing the specific probe WST that interacted with $NADH^+$ (nicotinamide adenine dinucleotide phosphate) resulting from NAD^+ (nicotinamide adenine dinucleotide) reduction by LDH to produce a yellow color was added to the collected medium. The released LDH was quantified by measuring the spectrophotometric absorbance at 450 nm using a Synergy H4 Hybrid microplate reader (BioTek Inc.).

Determination of Intracellular GSH Content. Intracellular GSH contents were determined using a commercially available kit (catalog no. 703002; Cayman Chemical Co., Ann Arbor, MI) according to the manufacturer's protocol. The assay uses glutathione reductase for the quantification of reduced GSH. The sulfhydryl group of GSH can react with 5,5′-dithio-bis-2-nitrobenzoic acid and results in a yellow 5-thio-2-nitrobenzoic acid. The mixed disulfide is reduced by glutathione reductase to recycle the GSH and produce more 5-thio-2-nitrobenzoic acid. The rate of 5-thio-2-nitrobenzoic acid production is directly proportional to this recycling reaction, which in turn is directly proportional to the concentration of reduced GSH in the sample. Briefly, HepG2 cells were deproteinized by adding 10% metaphosphoric acid, and total GSH levels were determined by a standard curve from known concentrations of reduced GSH. One portion of the cell pellet was dissolved in 1.0 M NaOH and analyzed for protein concentration using the Bio-Rad protein assay kit (Bio-Rad Laboratories). The absorbance of 5-thio-2-nitrobenzoic acid was measured at a wavelength of 412 nm using a Synergy H4 Hybrid microplate reader (BioTek Inc.).

TABLE 1

Predesigned primers used to determine human *PXR*, *CAR*, *HNF4α*, *DAX-1*, *PGC1α,* and *GAPDH* purchased from Integrated DNA Technologies Inc. (Coralville, IA)

The commercially available probes are prevalidated for accuracy by the vendor.

Assay ID (Catalog No.)	Gene	RefSeq	Transcripts Hit	Detects All Variants	Exon Location
Hs.PT.49a.18906856.g	*PXR/NR1I2*	Human	NM_033013	Yes	9–10
Hs.PT.49a.20642986	*CAR/NR1I3*	Human	NM_001077477	Yes	5–6
Hs.PT.56a.22913653	*HNF4α/NR2A1*	Human	NM_000457	Yes	4–6
Hs.PT.56a.1465041	*DAX1/NR0B1*	NM_000475	NM_000475	Yes	1–2
Hs.PT.56a.14965839	*PGC1α/PPARGC1A*	NM_013261	NM_013261	Yes	1–2
Hs.PT.39a.22214836	*GAPDH*	NM_002046	NM_002046	Yes	2–3

TABLE 2

miRNA probes used in this study

All probes are designed by Qiagen using the most up-to-date information from miRBase and prevalidated for accuracy by the vendor.

Detected Target	Catalog No.	Mature miRNA Sequence (5′→3′)	Product Name
miR-4666b	MS00040292	UUGCAUGUCAGAUUGUAAUUCCC	hsa-miR-4666b miScript Primer Assay
miR-561	MS00010192	CAAAGUUUAAGAUCCUUGAAGU	Hs_miR-561_2 miScript Primer Assay
miR-4477a	MS00041055	CUAUUAAGGACAUUUGUGAUUC	hsa-miR-4477a miScript Primer Assay
miR-3658	MS00023163	UUUAAGAAAACACCAUGGAGAU	Hs_miR-3658_1 miScript Primer Assay
U6 small nuclear RNA	MS00033740	GTGCTCGCTT CGGCAGCACA TATACTAAAA TTGGAACGAT ACAGAGAAGA TTAGCATGGC CCCTGCGCAA GGATGACACG CAAATTCGTG AAGCGTTCCA TATTTT	Hs_RNU6-2_1 miScript Primer Assay

Determination of Intracellular ROS Levels. Intracellular ROS levels were measured by a fluorometer using 2′,7′-dichlorofluorescein diacetate (DCFDA; Invitrogen Life Technologies Co.). The cell-permeant DCFDA passively diffuses into cells and is retained in the cells after deacetylation by intracellular esterases. Upon oxidation by hydroxyl, peroxyl, and other ROS, the nonfluorescent DCF is converted to the highly fluorescent 2′,7′-dichlorofluorescin. Briefly, HepG2 cells were cultured in a 96-well microplate at density of 1×10^4 cells/well. After transfection with the nontargeting control, miR-561 mimic or inhibitor with or without APAP treatment of 24 hours, the cells were incubated with 50 μM DCFDA (Invitrogen Life Technologies Co.) in Dulbecco's phosphate buffered saline for 30 minutes. Fluorescence intensity was analyzed at an excitation wavelength of 485 nm and emission wavelength of 530 nm using a Synergy H4 Hybrid microplate reader (BioTek Inc.).

RNA Interference of the *DAX-1* Gene. To knockdown the expression of *DAX-1* in primary human hepatocytes, DAX-1 small interfering RNA (siRNA) (catalog no. sc-35175; Santa Cruz Biotechnology Inc.) was added to the cells. The *DAX-1* siRNA is a pool of three target-specific 20- to 25-nuleotide siRNAs designed to knockdown *DAX-1*. Resuspension of the siRNA duplex in 330 μl of RNAse-free water made a 10 μM solution in a 10 μM Tris-HCl, pH 8.0, 20 mM NaCl, 1 mM EDTA-buffered solution.

Western Blotting Analysis. HepG2 cells or primary human hepatocytes were harvested and lysed with the lysis buffer (50 mmol HEPES at pH 7.5, 150 mmol NaCl, 10% glycerol, 1.5 mmol $MgCl_2$, 1% Triton-X 100, 1 mmol EDTA at pH 8.0, 10 mmol sodium pyrophosphate, 10 mmol sodium fluoride, and the protease inhibitor cocktail) and centrifuged at 3000*g* for 10 minutes at 4°C. Protein concentrations were measured by the Bio-Rad protein assay kit. An equal amount of a protein sample (30 μg) was separated on a 10% SDS-PAGE, and proteins were transferred onto immobilon polyvinylidene difluoride (PVDF) membrane (EMD Millipore Co., Billerica, MA) at 200 mA for 3 hours at 4°C. Blots were probed with the primary antibody. Immune complexes were detected using anti-mouse or anti-rabbit peroxidase-conjugated secondary IgG antibody (Boehringer Mannheim, Mannheim, Germany) and visualized using electrochemiluminescence Western blotting detection reagents (Amersham, now GE Healthcare, Piscataway, NJ). Protein level was normalized to the matching densitometric value of the internal control β-actin. Antibodies used in this study were as follows: rabbit IgG anti-DAX-1 antibody (K-17, catalog no. sc-841; Santa Cruz Biotechnology Inc.), rabbit polyclonal IgG anti-HNF4α antibody (H-171, cat. no. sc-8987; Santa Cruz Biotechnology Inc.), rabbit anti-PXR antibody (catalog no. AB10302; EMD Millipore Co.), mouse IgG anti-LXRα antibody (catalog no. ab41902; Abcam Inc., Cambridge, MA,), rabbit polyclonal IgG anti-FXR antibody (catalog no. sc-13063; H-130; Santa Cruz Biotechnology Inc.), rabbit polyclonal IgG anti-CAR antibody (catalog no. ab62590; Abcam Inc., Valencia, CA), rabbit IgG anti-PGC1α antibody (catalog no. 4259; Cell Signaling Technology Inc., Danvers, MA), and mouse IgG anti-β-actin antibody (catalog no. 3700S, 8H10D10; Cell Signaling Technology Inc.). β-Actin served as the internal control.

Chromatin Immunoprecipitation Assay. We conducted the chromatin immunoprecipitation (ChIP) assay to check whether miR-561 could modulate the binding or enrichment of HNF4α in complex with its coregulators to the promoter region of *PXR*. Briefly, HepG2 cells were transfected with the nontargeting control, miR-561 mimic, or inhibitor for 48 hours and treated with 5 mM APAP for 24 hours. APAP-treated cells were fixed with 1% *para*-formaldehyde in phosphate-buffered saline, and the cross-linking was stopped with 125 mM glycine at room temperature. Chromatin was sheared by sonication and immunoprecipitated with anti-DAX-1, anti-PGC1α, anti-HNF4α (all from Santa Cruz Biotechnology Inc.), or nonimmune IgG antibody at 4°C. Immune complexes were collected with protein A-Sepharose beads (Cell Signaling Technology Inc., MA). Total DNA was purified using a column method. The *PXR* promoter-specific primers that can detect HNF4α binding sites (see Supplemental Fig. 4) were used in PCR amplification [catalog no. GPH1009491(-)04A; Qiagen Inc.]. Samples were analyzed by 2% agarose gel electrophoresis and quantified relative to inputs using RT-PCR (Roche Diagnostics Co., Indianapolis, IN).

Statistical Analysis. Data are presented as the mean ± S.D. Multiple comparisons were evaluated by one-way analysis of variance (ANOVA) followed by Tukey's multiple comparison procedure, with $P < 0.05$ considered significant. All statistical tests were performed using Prism software version 6.0 (GraphPad Software Inc.).

Results

Prediction of miRNAs that May Regulate Human *DAX-1* and *HNF4α* Genes. Five miRNAs, including miR-561-3p (one of the two mature sequences of miR-561), miR-3658, miR-4477a, miR-4495, and miR-4666b, were predicted to regulate the human *DAX-1* gene by the miRBD program (Table 3). When the TargetScan program was applied, only one conserved miRNA, namely, miR-4495, was predicted to regulate *DAX-1*. However, at least 23 poorly conserved miRNAs, including miR-147, miR-217, miR-509-5p, miR-561, miR-644, miR-944, miR-3163, miR-3911, miR-4418, and miR-4793-3p, were predicted to affect the expression of *DAX-1* (Table 3). When MicroCosm/miRBase was used to search the miRNAs that possibly regulated *DAX-1*, about 50 miRNAs were found, including miR-561, miR-21, miR-297, and so forth. In addition, miRanda predicted that 53 miRNAs could regulate *DAX-1*, including miR-561, miR-656, miR-380, miR-3163, miR-3145, miR-137, miR-944, and so forth.

We also conducted a bioinformatics study using both TargetScan and miRBD to predict what miRNAs could regulate human *HNF4α* gene. TargetScan found a large number of nonconserved miRNAs that might regulate this gene (see Supplemental Table 1). These included miR-1, miR-16, miR-24, miR-150, miR-194, miR-378c, miR-454, miR-640, miR-1227, miR-1331, miR-2114, miR-3183, miR-4802-3p, and so forth. Only 24 poorly conserved miRNAs were predicted to regulate *HNF4α* by miRBD, including miR-661, miR-1202, miR-3188, miR-4270, and miR-4516 (see Supplemental Table 2). miRanda predicted 21 miRNAs that might regulate *HNF4α*, including miR-1, miR-24, miR-34a, miR-34c-5p, miR133a, miR-133b, miR-143, miR-150, miR-206, miR-216B, miR326, miR-328, miR-330-5p, miR-346, miR-361-5p, miR-382, miR-384, miR-449a, miR-449b, miR-485-5p, and miR-613. Notably, miR-561 was not predicted to regulate the human *HNF4α* gene by all these algorithms.

Prediction of the Gene Targets that May Be Regulated by miR-561. When TargetScan was used, miR-561 was predicted to regulate at least 774 conserved gene targets, with a total of 856 conserved sites and 619 poorly conserved sites (see Supplemental

TABLE 3

Predicted miRNAs that may regulate human *DAX-1* gene

Algorithm Used	Predicted miRNAs
miRBD/MirTarget2	**miR-561**, miR-3658, miR-4477a, miR-4495, miR-4666b
TargetScan	miR-147, miR-217, miR-509-3-5p, miR-509-5p, miR-548C-3p, **miR-561**, miR-581, miR-644, miR-663b, miR-944, miR-3136-3p, miR-3163, miR-3545-3p, miR-3653, miR-3658, miR-3664-5p, miR-3911, miR-4282, miR-4325, miR-4418, miR-4477a, miR-4495[a], miR-4714-5p, and miR-4793-3p
MiRanda	let-7f-1, miR-16-2, miR-17, miR-20a, miR-126, miR-137, miR-138-2, miR-147, miR-188-3p, miR-195, miR-200b, miR-200c, miR-216b, miR-217, miR-300, miR-301, miR-302b, miR-302d, miR-379, miR-380, miR-381, miR-411, miR-501, miR-507, miR-520d-5p, miR-524-5p, miR-548c-3p, miR-548n, miR-557, **miR-561**, miR-570, miR-581, miR-590-3p, miR-644, Mir-656, miR-663b, miR-1283, miR-19 and 75, miR-3118, miR-3145, miR-3148, miR-3163, miR-3118, miR-4282, miR-4325, miR-5481
MicroCosm/miRBase	let-7g, miR-19a, miR-19b, miR-20a, miR-21, miR-25, miR-31, miR-32, miR-92a, miR-92b, miR-126, miR-134, miR-135a, miR-147, miR-147b, miR-190b, miR-191, miR-217, miR-219-2-3p, miR-219-5p, miR-297, miR-300, miR-302b, miR-302d, miR-338-5p, miR-363, miR-367, miR-374a, miR-374b, miR-381, miR-452, miR-499-5p, miR-507, miR-520e, miR-544, miR-558, **miR-561**, miR-569, miR-581, miR-590-5p, miR-626, miR-630, miR-633, miR-644, miR-651, miR-654-5p, miR-656, miR-657, miR-672, miR-758, miR-801, miR-943, miR-944

[a] Conserved.

Table 3). These targets are mainly involved in cell proliferation and apoptosis, energy, and protein metabolism, signaling transduction and transport. Several NRs and corepressors were predicted to be regulated by miR-561, including NR1D2/ Rev-Erb-β receptor, the NR corepressors 1/NCOR1 and 7/NCOR7, NR2F2/chicken ovalbumin upstream promoter (COUP) transcription factor-like receptor, NR4A2/nuclear receptor related 1, and retinoid acid receptor-related orphan receptor A/RORA.

Our results showed that miRBD gave a larger number of targets that were predicted to be regulated by miR-561 compared with TargetScan (see Supplemental Table 4). There were 1514 gene targets that might be regulated by miR-561. Most of the predicted gene targets play a role in cell proliferation and apoptosis, energy, nuclear acid and protein metabolism, signaling transduction and transport. Four NRs were predicted to be regulated by miR-561, including DAX-1, Rev-erb-β/NR1D2, testicular receptor 2/NR2C1, and COUP/NR2F2 transcription factor-like receptor. Notably, CYP2U1 and 20A1 were also predicted to be regulated by miR-561.

We also searched the database using miRanda (http://www.microrna.org/microrna/) and found that miR-561 could regulate up to 8933 gene targets (data not shown), which is a much larger number than predicted by TargetScan and miRBD. These targets are mainly involved in cell growth regulation, energy, nucleic acid and protein metabolism, signaling transduction, transport, and apoptosis. NRs that were predicted to be regulated by miR-561 included Rev-erbβ, homolog of the *Drosophila* tail-less gene/NR2E1, COUP-transcription factor I, glucocorticoid receptor, nerve growth factor IB, neuron-derived orphan receptor 1/NR4A3, and liver receptor homolog-1/NR5A2.

APAP Induces the Expression of HNF4α, PXR, CAR, and PGC1α but Suppresses the Expression of DAX-1 in HepG2 Cells. APAP showed minor to moderate cytotoxicity toward only HepG2 cells, with an IC_{50} of 12.34 mM (see Supplemental Fig. 5). This value is comparable to those reported in the literature (Wang et al., 2002; Kostrubsky et al., 2005).

Activation of PXR, as well as CAR, represents an important mechanism for the induction of CYP3A4 that can convert APAP to its toxic metabolite, NAPQI (Hinson et al., 2010). HNF4α determines PXR- and CAR-mediated induction of CYP3A4 in human hepatocytes, serving as an important regulator of NR-mediated response to xenobiotics exposure (Tirona et al., 2003). Thus, we investigated the activation of these key NRs in HepG2 cells in response to APAP treatment. In HepG2 cells, HNF4α (as a band of ~54 kDa), PXR (as a band of ~49 kDa), CAR (as a band of ~45 kDa), FXR (as a band of ~69 kDa), and LXRα (as a band of ~50 kDa) were all detected at low to moderate levels; DAX-1 was also readily detected as a single band of ~60 kDa, and PGC1α was shown as a band of ~130 kDa (Fig. 1A). In previous studies, DAX-1 was also detected in HepG2 cells (Nedumaran et al., 2009, 2010).

As shown in Fig. 1, A and B, APAP significantly increased HNF4α, PXR, and CAR protein levels in a concentration-dependent manner in HepG2 cells (Fig. 1, A and B). APAP at 1, 5, and 10 mM increased the expression level of HNF4α protein in HepG2 cells by 62.8, 100.1, and 124.1% ($P < 0.01$ or 0.001, by one-way ANOVA), respectively, compared with control cells but APAP at a lower concentration (0.5 mM) did not significantly affect the expression of HNF4α in HepG2 cells (Fig. 1, A and B). For PXR, APAP only at 5 and 10 mM enhanced its expression by 54.5% and 142.5% ($P < 0.001$; Fig. 1, A and B), respectively, compared with control cells. Lower concentrations of APAP (0.5 and 1 mM) did not significantly change PXR levels. In addition, APAP at 1, 5, and 10 mM increased the expression of CAR by 33.8%, 82.6%, and 92.1% ($P < 0.001$; Fig. 1, A and B), respectively, compared with control cells. Increased levels of these important NRs by APAP exposure indicate that the activation of HNF4α, and subsequently activation of PXR and CAR, is involved in APAP-induced cytotoxicity in HepG2 cells. It appears that a low concentration of APAP (1 mM) could activate HNF4α and CAR, but not PXR. A lower concentration of APAP (0.5 mM) did not activate HNF4α, PXR, or CAR, suggesting that the cells did not need to activate these NRs to protect them from the potential toxicity of APAP when the hepatocytes could efficiently remove NAPQI at subtoxic levels of APAP.

Basal expression of both FXR and LXRα was readily detected in HepG2 cells (Fig. 1A). Our study showed that treatment of HepG2 cells with APAP at 0.5 or 1 mM increased the expression level of FXR by 3.5% and 16.8% ($P > 0.05$), respectively; but treatment of HepG2 cells with APAP at 5 or 10 mM decreased the expression level of FXR by 29.3% and 69.0% ($P > 0.05$), respectively, compared with control

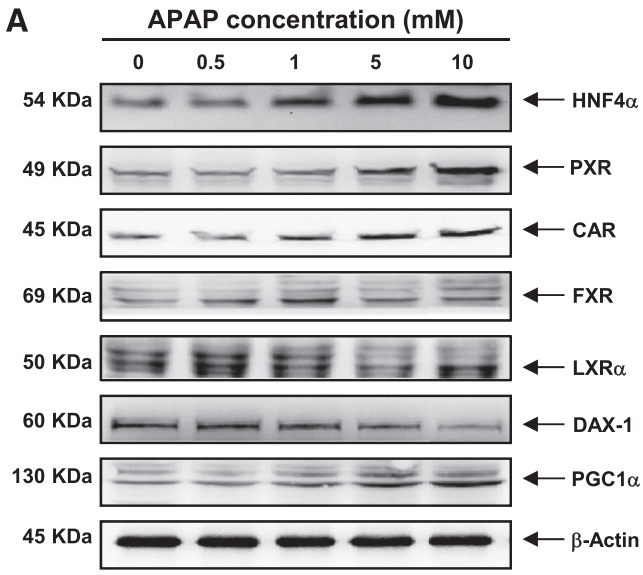

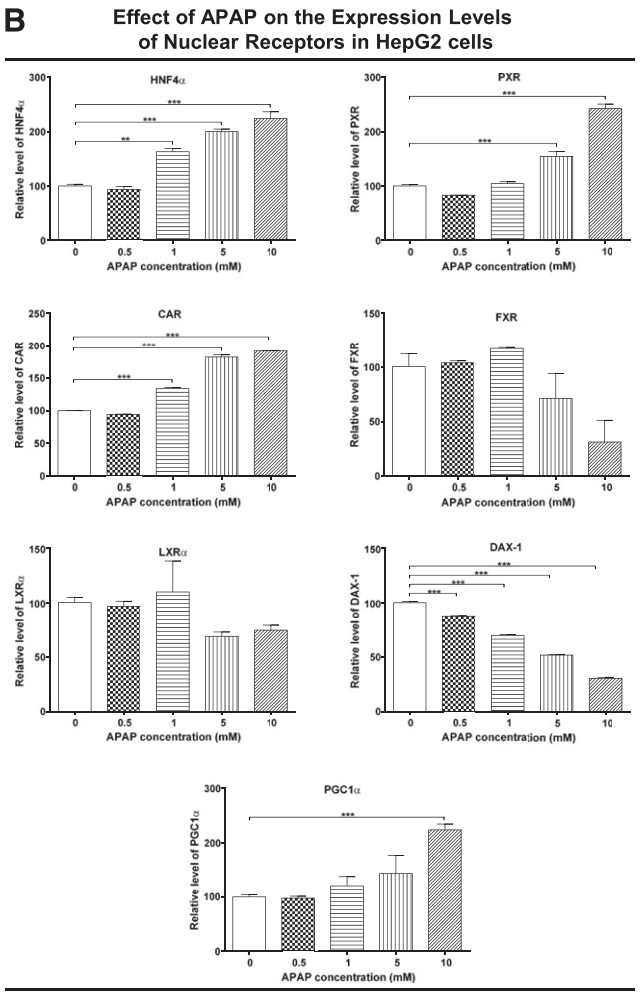

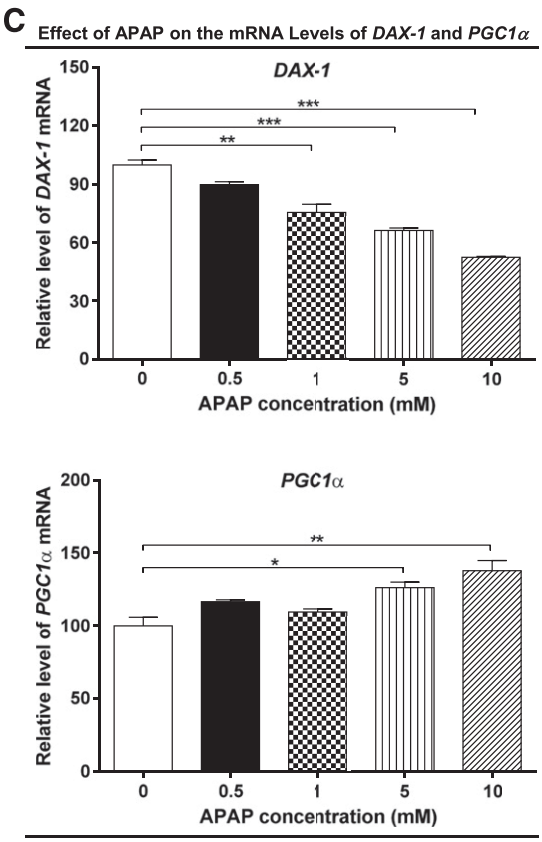

Fig. 1. (A and B) Effects of APAP treatment on the protein expression levels of HNF4α, PXR, CAR, FXR, LXRα, DAX-1, and PGC1α in HepG2 cells. HepG2 cells were treated with APAP at 0.5, 1, 5, and 10 mM for 24 hours, and cell lysates were prepared using the RIPA buffer. Total cell lysates were separated on a 10% SDS-PAGE, transferred to a PVDF membrane, and immunoblotted with the specific antibody against HNF4α, PXR, CAR, FXR, LXRα, DAX-1, or PGC1α. (A) Representative blots of the target proteins. (B) Bar graphs showing the relative blot intensity of HNF4α, PXR, CAR, FXR, LXRα, DAX-1, and PGC1α. β-Actin expression was monitored as an internal control. (C) Effect of APAP treatment on the mRNA levels of *DAX-1* and *PGC1*α genes in HepG2 cells. Cells were treated with 0.5, 1, 5, or 10 mM APAP for 24 hours. First-stranded cDNA was synthesized from the total RNA, and quantitative RT-PCR was conducted with gene-specific probes. *GAPDH* mRNA served as the internal control. The results are from at least three independent experiments. $^{*}P < 0.05$; $^{**}P < 0.01$; $^{***}P < 0.001$; by one-way ANOVA and Tukey's post hoc test to compare the protein and mRNA levels of the nuclear receptors with those of control cells.

cells. Similarly, treatment of HepG2 cells with APAP at 1 mM increased the expression level of LXRα by 9.7% ($P > 0.05$), but treatment of HepG2 cells with APAP at 0.5, 5, or 10 mM decreased the expression level of LXRα by 3.4%, 31.0%, and 25.2% ($P > 0.05$), respectively, compared with control cells (Fig. 1, A and B). FXR is expressed at high levels in the liver, intestine, kidney, and adrenal glands, with chenodeoxycholic acid and other bile acids being its natural ligands (Jonker et al., 2012). FXR regulates cholesterol, bile acid, lipoprotein, glucose metabolism, liver regeneration, innate immunity, and inflammation. LXRα and LXRβ are important regulators of cholesterol, fatty acid, and glucose homeostasis (Jakobsson et al., 2012). Activation of Lxr in mice increases APAP clearance through induction of phase II enzymes and abolishes its hepatotoxicity (Saini et al., 2011). On activation, FXR and LXR translocate to the nucleus, form a heterodimer with 9-*cis* retinoic acid receptor (RXR), and bind to response elements on the promoter of target genes (Jonker et al., 2012). *Fxr* gene dosage is positively correlated with the degree of protection from APAP-induced hepatotoxicity in mice, and pretreatment of mice with an FXR agonist, GW4064 (3-(2,6-dichlorophenyl)-4-(3′-carboxy-2-chlorostilben-4-yl)oxymethyl-5-isopropylisoxazole), provides significant protection from APAP-induced hepatotoxicity (Lee et al., 2010). Our results demonstrate that APAP at low to high concentrations does not significantly induce the expression of both LXRα and FXR in HepG2 cells, suggesting a minor or less important role of these two nuclear receptors in APAP-induced hepatotoxicity.

The expression levels of DAX-1 and PGC1α in HepG2 cells were also altered by APAP treatment. As shown in Fig. 1A and B, APAP significantly decreased the expression level of DAX-1 in HepG2 cells in a concentration-dependent manner ($P < 0.001$, by one-way ANOVA). Treatment of HepG2 cells with APAP at 0.5, 1, 5, or 10 mM decreased the expression level of DAX-1 by 12.3%, 30.0%, 48.1%, and 69.5% ($P < 0.001$, by one-way ANOVA; Fig. 1, A and B), respectively, compared with control cells. In addition, treatment of HepG2 cells with APAP at 10 mM increased the expression level of PGC1α by 123.2% ($P < 0.001$; Fig. 1, A and B). Treatment of HepG2 cells with APAP at 1 or 5 mM increased the expression level of PGC1α by 20.2 and 42.8% ($P > 0.05$; Fig. 1, A and B). These results demonstrate that APAP exposure induced PGC1α expression but suppressed the expression of DAX-1 in HepG2 cells. The reason for the differential response of DAX-1 and PGC1α to distinct concentrations of APAP (0.5–5 mM) is unknown. The *DAX-1* gene appears to be downregulated rapidly by low to high concentrations of APAP, whereas the *PGC1α* gene is upregulated only when the hepatocytes are treated with higher concentrations of APAP.

APAP Treatment Does Not Alter the mRNA Levels of the *HNF4α*, *PXR*, and *CAR* Genes in HepG2 Cells. To determine whether the enhanced NR protein expression caused by APAP treatment was mediated by post-transcriptional or transcriptional modification, we investigated the mRNA levels of *HNF4α*, *PXR*, and *CAR* in HepG2 cells treated with APAP at 0.5–10 mM. As shown in Supplemental Fig. 6, no significant changes were noted in the mRNA levels of *HNF4α*, *PXR*, and *CAR* on APAP treatment for 24 hours in HepG2 cells ($P > 0.05$ by one-way ANOVA). Treatment of HepG2 cells with APAP at 1–10 mM increased the mRNA levels of *HNF4α*, *PXR*, and *CAR* by 9.7%–19.0%, 20.9%–27.6%, and 18.1%–28.0%, respectively, compared with control cells ($P > 0.05$). These data suggested that induction of HNF4α, PXR, and CAR protein expression by APAP was mediated by post-transcriptional modification only.

APAP Treatment Alters the Expression of *DAX-1* and *PGC1α* mRNAs in HepG2 Cells. We found that APAP treatment significantly induced the expression of PGC1α but decreased that of DAX-1 in HepG2 cells. We further investigated the effects of 0.5–10 mM APAP treatment on the mRNA levels of *DAX-1* and *PGC1α* in HepG2 cells. In HepG2 cells, *DAX-1* and *PGC1α* mRNAs were remarkably detected by RT-PCR analysis under basal conditions (Fig. 1C). Treatment of APAP significantly suppressed the expression level of *DAX-1* mRNA in a concentration-dependent manner ($P < 0.01$ or 0.001 by one-way ANOVA; Fig. 1C). Treatment of APAP at 1, 5, and 10 mM reduced the expression level of *DAX-1* mRNA by 24.5%, 33.8%, and 47.6% ($P < 0.01$ or 0.001), respectively, compared with control cells. APAP at 0.5 mM did not significantly affect the mRNA levels of *DAX-1* in HepG2 cells. In contrast, treatment with APAP significantly increased the level of *PGC1α* mRNA in a concentration-dependent manner in HepG2 cells ($P < 0.05$ or 0.01 by one-way ANOVA; Fig. 1C). Treatment of APAP at 5 and 10 mM increased the expression level of *DAX-1* mRNA by 26.3% and 37.9% ($P < 0.05$ or 0.01), respectively, compared with control cells. Treatment of APAP at 0.5 and 1 mM only slightly increased the mRNA levels of *PGC1α* in HepG2 cells ($P > 0.05$). These data indicate that APAP at relatively high concentrations significantly alters the expression of *DAX-1* and *PGC1α* genes, whereas neither gene was very sensitive to low concentrations of APAP. This is important for the cells to retain their energy when they encounter a low level of xenobiotics that can be efficiently eliminated from the cells.

HNF4α Is Physically Associated with DAX-1 in HepG2 Cells Exposed to APAP. In the following study, we first examined the possible interaction of HNF4α with DAX-1 by performing the coimmunoprecipitation assay in HepG2 cells. Agarose-conjugated IgG was used as the negative control in immunoprecipitation (IP). As shown in Fig. 2A, incubation of cell lysates with the control IgG in IP did not detect any target proteins in the following immunoblotting assay. In non-IP input controls, DAX-1 and HNF4α were detected when corresponding primary antibody was used in the immunoblotting assay. When the primary antibody against DAX-1 first precipitated DAX-1 present in cell lysates, HNF4α was detected in the subsequent immunoblotting assay for the eluted target protein complex (Fig. 2A). The HNF4α protein level determined in the immunoblotting assay was significantly decreased in a concentration-dependent manner ($P < 0.001$, by one-way ANOVA; Fig. 2, A and B). Treatment of HepG2 cells with APAP at 0.5, 1, or 5 mM for 24 hours decreased the cellular lysate HNF4α level by 18.4%, 60.9%, and 82.0% ($P < 0.001$; Fig. 2, A and B), respectively, compared with control cells treated with the control vehicle only. Use of one single antibody against HNF4α in both immunoprecipitation and immunoblotting detected HNF4α only in cell lysates ($P < 0.001$; Fig. 2, A and B). Treatment of HepG2 cells with APAP at 1 or 5 mM for 24 hours increased cellular lysate HNF4α level by 55.0 and 42.9% ($P < 0.001$; Fig. 2, A and B), respectively, compared with control cells treated with the control vehicle only. However, treatment of HepG2 cells with APAP at 0.5 mM for 24 hours only slightly decreased cellular lysate HNF4α level by 14.3% ($P > 0.05$).

On the other hand, when the primary antibody against HNF4α first precipitated HNF4α present in cell lysates, DAX-1 was detected in the subsequent immunoblotting assay for the eluted target protein complex (Fig. 2A). The DAX-1 protein level determined in the immunoblotting assay was significantly decreased in a concentration-dependent manner ($P < 0.001$, by one-way ANOVA; Fig. 2, A and B). Treatment of HepG2 cells with APAP at 0.5, 1, or 5 mM for 24 hours decreased cellular lysate DAX-1 level by 45.1%, 60.2%, and 51.2% ($P < 0.001$; Fig. 2, A and B), respectively, compared with control cells treated with the control vehicle only. Use of one single antibody against DAX-1 in both immunoprecipitation and immunoblotting detected DAX-1 only in cell lysates ($P < 0.001$; Fig. 2, A and B). Treatment of HepG2 cells with

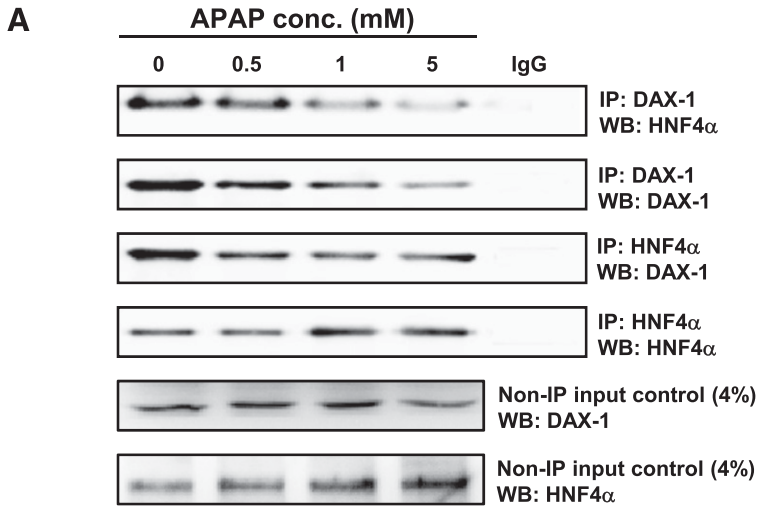

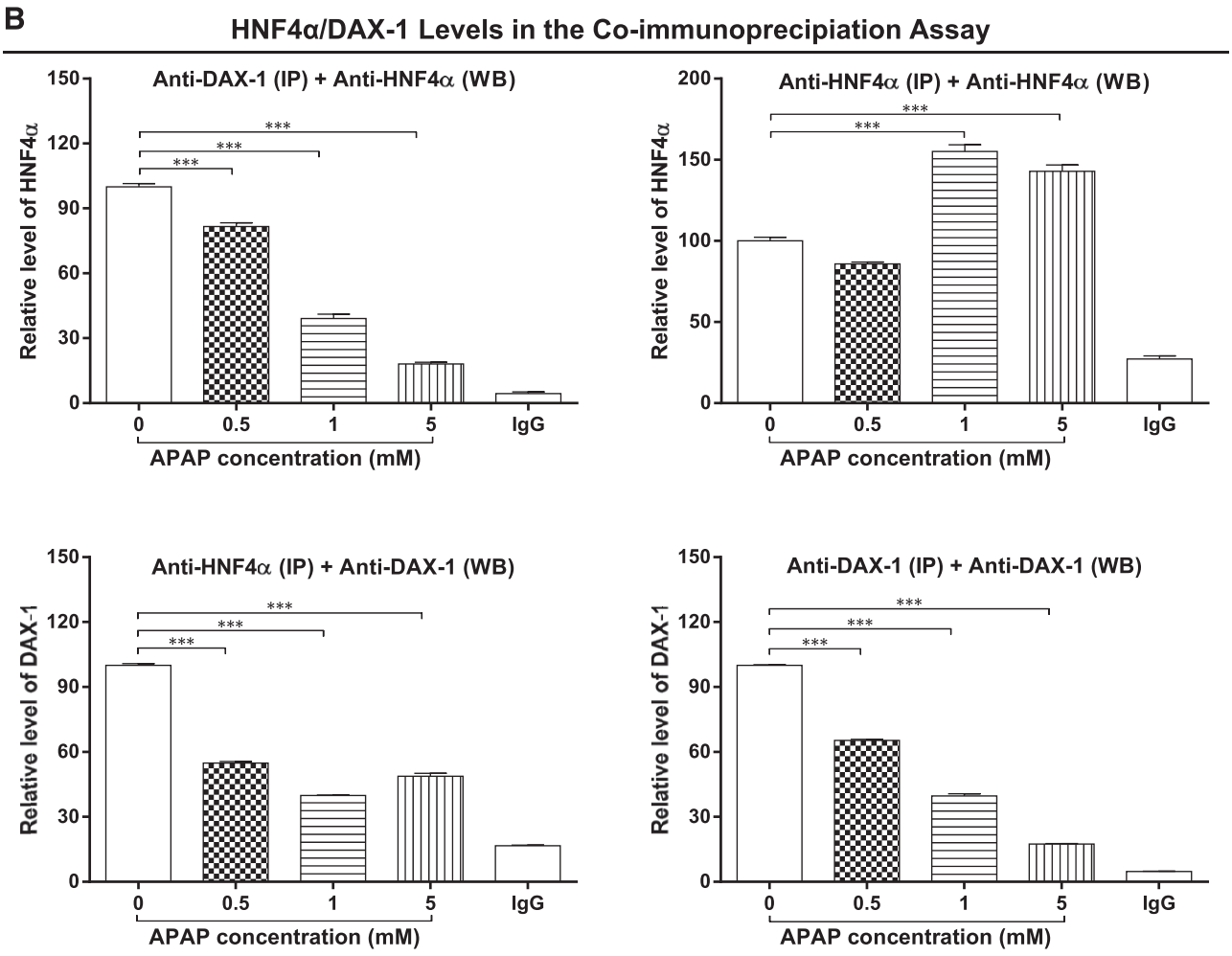

Fig. 2. (A) Representative blots of the coimmunoprecipitation assay in HepG2 cells treated with APAP at 0.5, 1, or 5 mM for 24 hours. Cells were harvested and lysed, and total cellular lysates were first subjected to immunoprecipitation (IP) with anti-DAX-1 or anti-HNF4α antibody. The bound target protein was then washed and eluted, subjected to Western blotting assay (WB) with antibodies against HNF4α or DAX-1. (B) Bar graphs showing the relative band intensity of HNF4α or DAX-1. β-Actin was used as the internal control. The results are from at least three independent experiments. $^{***}P < 0.001$; by one-way ANOVA and Tukey's post hoc test to compare DAX-1/HNF4α levels with the control cells.

APAP at 0.5, 1, or 5 mM for 24 hours decreased cellular lysate DAX-1 level by 34.6%, 60.3%, and 82.5% ($P < 0.001$; Fig. 2, A and B), respectively, compared with control cells treated with the control vehicle only.

These findings demonstrated that the rabbit primary antibody against HNF4α coprecipitated with DAX-1, and vice versa, the rabbit primary antibody against DAX-1 coprecipitated with HNF4α in HepG2 cells upon APAP treatment, which was detected in the following

immunoblotting assay. HNF4α is physically associated with DAX-1 in HepG2 cells exposed to APAP.

APAP Upregulates miR-561 in HepG2 Cells. To identify miRNAs that may play a role in regulating *DAX-1,* the expression levels of several miRNAs that are possibly involved in the regulation of *DAX-1* mRNA based on our bioinformatics data using both TargetScan and miRBD algorithms (see Supplemental Tables 1 and 2) were examined. No significant changes were observed in the expression levels of miR-4666b, miR-4477, and miR-3658 in HepG2 cells exposed to APAP at concentrations from 0.5 to 5.0 mM for 24 hours ($P > 0.05$ by one-way ANOVA; see Supplemental Fig. 7). Treatment of HepG2 cells with 5 mM APAP for 24 hours increased the level of miR-4666b, miR-4477, and miR-3658 by 37.4%, 29.0%, and 5.4%, respectively, compared with the corresponding control cells ($P > 0.05$).

As shown in Fig. 3A, APAP treatment increased the miR-561 level in a concentration-dependent manner in HepG2 cells. Treatment of HepG2 cells with 1 or 5 mM APAP for 24 hours increased the miR-561 level by 148.2% and 402.7% ($P < 0.05$ or 0.001 by one-way ANOVA), respectively, compared with control cells. Treatment of HepG2 cells with 0.5 mM APAP for 24 hours only slightly increased the miR-561 level by 16.3% ($P > 0.05$ by one-way ANOVA). These data indicate that induction of miR-561 is relatively specific and remarkable when HepG2 cells are treated with APAP.

Antioxidants Reverse APAP-Induced miR-561 Induction in HepG2 Cells. We used several common antioxidants including *N*-acetyl-L-cysteine (NAC), vitamin C, and GSH to determine whether oxidative stress was involved in APAP-induced miR-561 induction in HepG2 cells. Treatment of HepG2 cells with NAC at 5 mM, vitamin C at 100 μM, or GSH at 1 mM alone did not alter the levels of miR-561. As shown in Fig. 3B, NAC at 5 mM, vitamin C at 100 μM, and GSH at 1 mM suppressed the inducing effect of APAP on miR-561 by 49.2%, 47.8%, and 67.7% ($P < 0.05$ for NAC and vitamin C; $P < 0.01$ for GSH by one-way ANOVA), respectively, compared with control cells receiving 5 mM APAP alone. These data suggest that oxidative stress generated by APAP treatment may be partially responsible for the ability of APAP to induce miR-561 in HepG2 cells.

Overexpression and Knockdown of miR-561 Alter the DAX-1-3′-UTR Luciferase Reporter Activity. In general, miRNAs function as post-transcriptional regulators of target gene expression. To investigate the role of miR-561 in the transcriptional regulation of *DAX-1* in HepG2 cells, we used a reporter gene vector containing a luciferase gene followed by the 3′-UTR of human *DAX-1* mRNA (DAX-1-3′-UTR). Overexpression of miR-561 decreased DAX-1-3′-UTR reporter activity by 54.1% in HepG2 cells ($P < 0.001$ by one-way ANOVA; Fig. 3C) compared with control cells transfected with the nontargeting miRNA. In contrast, transfection of miR-561 inhibitor increased DAX-1-3′-UTR reporter activity by 68.5% ($P < 0.001$ by one-way ANOVA; Fig. 3C). As expected, treatment of 5 mM APAP decreased DAX-1-3′-UTR reporter activity by 68.3% ($P < 0.001$ by one-way ANOVA) and transfection of miR-561 inhibitor restored APAP-mediated suppression of DAX-1-3′-UTR reporter activity by 112.2% in HepG2 cells ($P < 0.05$ by one-way ANOVA; Fig. 3C) compared with control cells treated with 5 mM APAP alone. Transfection of miR-561 mimic further decreased APAP-mediated suppression of DAX-1-3′-UTR reporter activity by 55.6% in HepG2 cells, but it did not achieve statistical significance ($P > 0.05$ by one-way ANOVA). These data suggest that DAX-1 is a target of miR-561 and that miR-561-induced decreased expression of DAX-1 is through post-transcriptional mechanism.

To check the specificity of the miR-561 mimic and inhibitor, we investigated the expression levels of miR-561 and miR-4477 when treated with miR-561 mimic or inhibitor in HepG2 cells. As shown in Supplemental Fig. 8, treatment of miR-561 mimic for 24 hours increased the miR-561 expression level 253-fold in HepG2 cells ($P < 0.001$ by one-way ANOVA). Treatment of miR-561 inhibitor decreased miR-561 expression by 46.3% in HepG2 cells, but it did not achieve statistical significance. Remarkably, no significant change occurred in miR-4477 expression levels by either miR-561 mimic or inhibitor treatment in HepG2 cells. These findings indicate the specificity and selectivity of miR-561 mimic and inhibitor and that the moderate suppressing effect of miR-561 inhibitor may imply a remarkable basal or constitutive expression of miR-561 in HepG2 cells.

miR-561 Promotes APAP-Induced LDH Release, ROS Generation, and GSH Depletion in HepG2 Cells. To determine whether miR-561 modulated APAP-induced hepatotoxicity, we examined the LDH release, ROS generation, and GSH depletion in HepG2 cells transfected with nontargeting control, miR-561 mimic, or miR-561 inhibitor with or without APAP treatment at 5.0 mM. These represent hepatotoxic markers related to enzyme leakage resulting from cellular injury and oxidative stress.

As shown in Fig. 4A, treatment of HepG2 cells by transfection with miR-561 mimic increased LDH release by 44.4% compared with control cells ($P < 0.01$ by one-way ANOVA), whereas transfection with miR-561 inhibitor only slightly reduced LDH release from HepG2 cells by 18.3% compared with control cells ($P > 0.05$). Treatment of HepG2 cells with 5 mM APAP enhanced LDH release by 69.1% ($P < 0.001$ by one-way ANOVA). When HepG2 cells were treated with APAP plus transfection with the miR-561 mimic, the LDH release was only slightly increased by 13.6% compared with control cells receiving 5 mM APAP alone ($P > 0.05$ by one-way ANOVA). Treatment of 5 mM APAP plus transfection of a miR-561 inhibitor into HepG2 cells decreased the release of LDH by 22.8% compared with control cells treated with 5 mM APAP only ($P < 0.05$ by one-way ANOVA; Fig. 4A). These data indicate that miR-561 overexpression can enhance APAP-induced LDH release, and miR-561 knockdown reduces the enzyme leakage from HepG2 cells exposed to APAP.

ROS generation has been associated with APAP-induced liver injuries (Hinson et al., 2010). Therefore, we examined the effects of miR-561 overexpression and knockdown on APAP-induced ROS production in HepG2 cells. Treatment of HepG2 cells with miR-561 mimic transfection increased ROS levels by 23.1% ($P < 0.001$ by one-way ANOVA), but transfection with miR-561 inhibitor decreased ROS generation by 26.4% in HepG2 cells compared with control cells with nontargeting control transfection ($P < 0.001$ by one-way ANOVA; Fig. 4B). Treatment of HepG2 cells with 5 mM APAP increased ROS production by 51.6% ($P < 0.001$ by one-way ANOVA; Fig. 4B). When APAP-treated HepG2 cells were cotreated with miR-561 mimic transfection, the ROS level was increased by 21.5% ($P < 0.001$ by one-way ANOVA) compared with control cells treated with APAP alone. Treatment of APAP-treated HepG2 cells with miR-561 inhibitor transfection decreased ROS level by 32.7% compared with control cells receiving APAP alone ($P < 0.001$ by one-way ANOVA; Fig. 4B). These data indicate that miR-561 overexpression can increase basal and APAP-induced ROS generation, whereas miR-561 knockdown reduces basal and APAP-induced ROS production in HepG2 cells.

GSH depletion is one of the major mechanisms in APAP-induced hepatotoxicity (Saito et al., 2010). Our further study showed that transfection of HepG2 cells with the miR-561 mimic augmented GSH depletion by 23.0% ($P < 0.001$ by one-way ANOVA; Fig. 4C). However, transfection of HepG2 cells with the miR-561 inhibitor

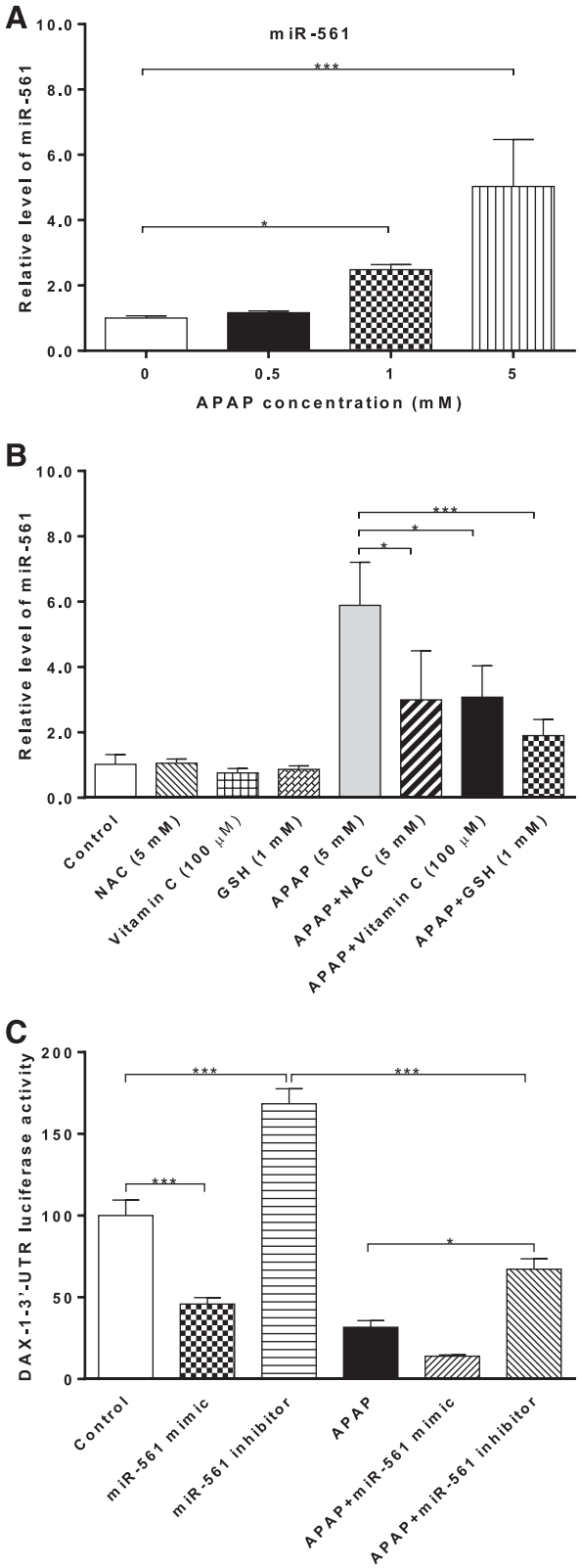

Fig. 3. (A) Effect of APAP treatment on the expression level of miR-561 in HepG2 cells. Cells were treated with APAP at 0.5, 1, or 5 mM for 24 hours, and the miR-561 level was measured using quantitative RT-PCR. (B) Effect of antioxidants on APAP-induced miR-561 upregulation in HepG2 cells. HepG2 cells were preincubated with NAC at 5 mM, vitamin C at 100 μM, or GSH at 1 mM for 1 hour followed by treatment with APAP at 5 mM for 24 hours. The miR-516 level was measured using the miScript assay system. (C) Effect of miR-561 knockdown and overexpression on DAX-1-3′-UTR reporter activity in HepG2 cells. HepG2 cells were transfected with a DAX-1-3′-UTR reporter and nontargeting control, miR-561 mimic, miR-561 inhibitor, or β-galactosidase (as the internal control). APAP at 0.5, 1, or 5 mM was added and incubated for 24 hours. Thereafter, cells were harvested, and luciferase and β-galactosidase activities were determined. Data are the mean ± S.D. of at least three independent experiments. *$P < 0.05$; ***$P < 0.001$; by one-way ANOVA and Tukey's post hoc test to compare miR-561 levels or DAX-1-3′-UTR luciferase activity with the corresponding control cells.

reduced GSH depletion by 10.3% compared with control cells transfected with the nontargeting miRNA ($P < 0.05$ by one-way ANOVA; Fig. 4C). Treatment of HepG2 cells with 5 mM APAP increased GSH depletion by 17.9% ($P < 0.01$ by one-way ANOVA; Fig. 4C). When APAP-treated HepG2 cells were transfected with the miR-561 mimic, the GSH level was reduced by 21.8% compared with control cells treated with APAP lone ($P < 0.01$ by one-way ANOVA; Fig. 4C). In contrast, transfection of APAP-treated HepG2 cells with the miR-561 inhibitor increased GSH production by 23.0% compared with control cells treated with APAP alone ($P < 0.01$ by one-way ANOVA; Fig. 4C). These data indicate that miR-561 overexpression can worsen basal and APAP-induced GSH depletion, whereas miR-561 knockdown reduces basal and APAP-induced GSH depletion in HepG2 cells.

The aforementioned results clearly demonstrate that miR-561 deteriorates APAP-induced cytotoxicity in HepG2 cells exposed to APAP through enhanced LDH release, generation of ROS, and depletion of intracellular GSH. This may represent an additional pathway that miR-561 modulates APAP-induced hepatotoxicity. These harmful effects of miR-561 on hepatocytes exposed to APAP are highly likely to be associated with NR activation.

Overexpression and Knockdown of miR-561 Alter the Expression of HNF4α, PXR, CAR, DAX-1, and PGC1α in HepG2 Cells and Primary Human Hepatocytes. Our data suggest that APAP-induced activation or upregulation of PXR and CAR was regulated by HNF4α, which physically interacted with DAX-1 in HepG2 cells. Next, to examine the role of miR-561 in APAP-induced PXR/CAR activation, we tested whether the expression of these NRs was affected by transfection of nontargeting control, miR-561 mimic, or miR-561 inhibitor into HepG2 cells and primary human hepatocytes.

When HepG2 cells were treated with 5 mM APAP for 24 hours, the expression level of PXR, CAR, HNF4α, and PGC1α was increased by 40.5%, 53.9%, 36.5%, and 31.7% ($P < 0.05$, 0.01, or 0.001 by one-way ANOVA; Fig. 5, A and B), whereas the level of DAX-1 was decreased by 50.8% compared with control cells ($P < 0.001$). Transfection of miR-561 mimic into HepG2 cells increased the expression level of PXR by 26.2% compared with control cells transfected with the nontargeting miRNA ($P < 0.001$ by one-way ANOVA; Fig. 5, A and B). Transfection of miR-561 mimic into APAP-treated HepG2 cells also increased the level of PXR by 22.3% compared with control cells treated with 5 mM APAP alone ($P < 0.001$ by one-way ANOVA; Fig. 5, A and B). In contrast, transfection of miR-561 inhibitor into HepG2 cells downregulated the basal and APAP-induced expression of PXR by 29.2% and 36.7%, respectively, compared with control cells ($P < 0.001$; Fig. 5, A and B).

The APAP-induced expression level of CAR was increased by 43.8% upon miR-561 mimic transfection into HepG2 cells compared with the control cells receiving APAP alone ($P < 0.05$) but only slightly increased the basal expression of this nuclear receptor by 22.0% ($P > 0.05$) in HepG2 cells subjected to miR-561 mimic transfection (Fig. 5, A and B). On the contrary, transfection of miR-561 inhibitor into HepG2 cells decreased the basal and APAP-induced

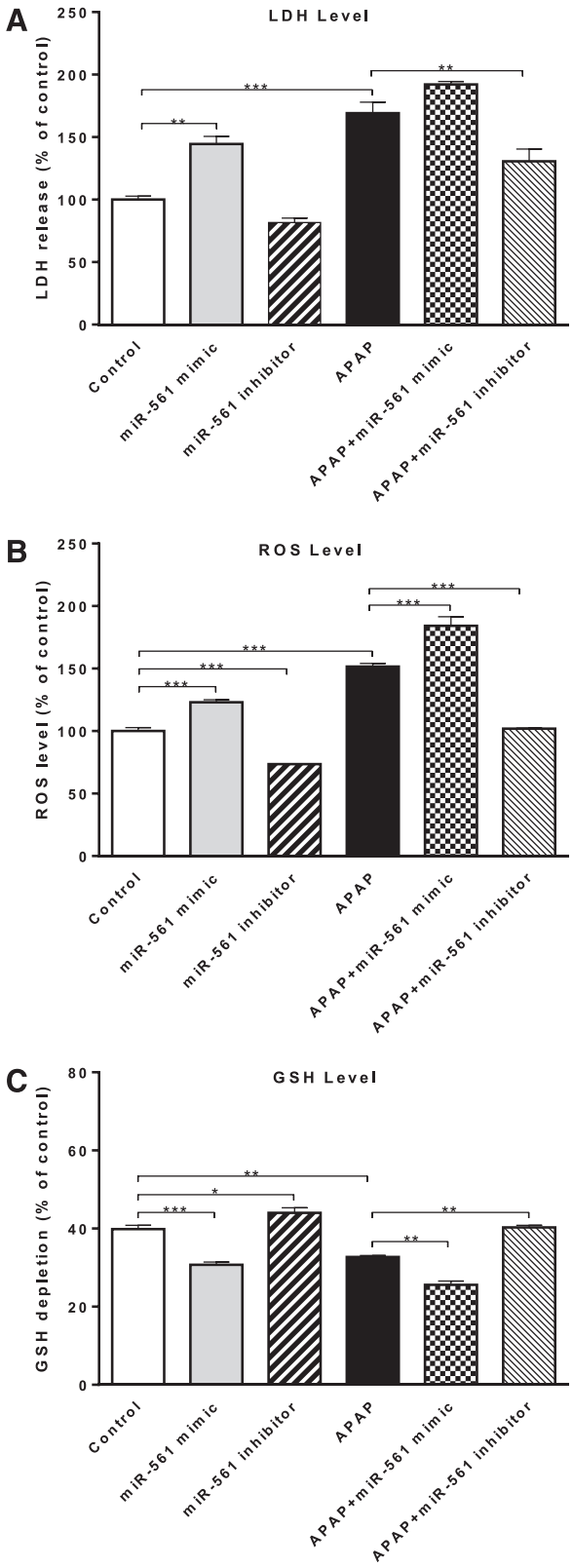

Fig. 4. Effect of overexpression or knockdown of miR-561 on APAP-induced LDH release, ROS generation, and GSH depletion in HepG2 cells. HepG2 cells were transfected with nontargeting control, miR-561 mimic, or miR-561 inhibitor for 48 hours. APAP at 5 mM was added to the cells and incubated for 24 hours after transfection. (A) LDH release was monitored using a commercially available kit. (B) Intracellular ROS levels were measured by incubating the cells with 50 μM DCF-DA for 30 minutes, and fluorescence intensity was analyzed using a microplate fluorescence reader. (C) Total reduced GSH content was determined using a commercially available kit. The results are from at least three independent experiments. $^*P < 0.05$; $^{**}P < 0.01$; $^{***}P < 0.001$; by one-way ANOVA and Tukey's post hoc test to compare LDH leakage and intracellular ROS and GSH levels with the control cells.

expression level of CAR by 51.8% and 36.4%, respectively, compared with control cells ($P < 0.05$; Fig. 5, A and B).

DAX-1-mediated HNF4α activation determines PXR and CAR activation (McCabe, 2007). Thus, we further examined the role of miR-561 in the regulation of HNF4α, DAX-1, and PGC1α at basal conditions and under APAP exposure. Transfection of miR-561 mimic into HepG2 cells did not affect basal HNF4α expression and only slightly enhanced the APAP-induced activation of HNF4α by 17.3% ($P > 0.05$ by one-way ANOVA; Fig. 5, A and B). In contrast, transfection of miR-561 inhibitor into HepG2 cells suppressed the basal and APAP-induced activation of HNF4α by 83.7% and 34.7%, respectively, compared with control cells ($P < 0.001$ by one-way ANOVA; Fig. 5, A and B).

As shown in Fig. 5, A and B, transfection of the miR-561 mimic into HepG2 cells decreased the basal expression level of DAX-1 by 43.2% ($P < 0.001$ by one-way ANOVA) and reduced the DAX-1 level by 20.8% in APAP-treated HepG2 cells subject to transfection of the miR-561 mimic ($P < 0.001$ by one-way ANOVA). Transfection of the miR-561 inhibitor into HepG2 cells only slightly enhanced the basal expression of DAX-1 by 9.0% ($P > 0.05$) but increased the DAX-1 level by 125.8% in APAP-treated HepG2 cells subjected to transfection of the miR-561 inhibitor ($P < 0.001$ by one-way ANOVA; Fig. 5, A and B). With regard to PGC1α, transfection of the miR-561 inhibitor into HepG2 cells suppressed the basal and APAP-induced activation of PGC1α by 64.0% and 16.3%, respectively, compared with control cells ($P < 0.001$ by one-way ANOVA; Fig. 5, A and B). However, transfection of the miR-561 mimic into HepG2 cells did not significantly affect basal and APAP-induced activation of PGC1α ($P > 0.05$ by one-way ANOVA; Fig. 5, A and B).

Overall, these data from HepG2 cells demonstrate that miR-561 overexpression via its mimic transfection significantly enhances basal and APAP-induced expression of PXR and CAR and significantly suppresses the basal and APAP-induced expression of DAX-1 but did not significantly affect basal and APAP-induced expression of HNF4α and PGC1α. Knockdown of miR-561 using the miR-561 inhibitor transfection downregulates basal and APAP-induced HNF4α, PXR, CAR, and PGC1α expression but upregulates DAX-1 expression in HepG2 cells exposed to APAP. The effect of miR-561 on the expression of these NRs and corepressors is differential, depending on basal or APAP-exposed conditions and other factors in HepG2 cells. APAP-induced transactivation of HNF4α, PXR, CAR, and PGC1α may be mediated, at least in part, through miR-561 induction and subsequently DAX-1 inhibition in HepG2 cells.

To further investigate and confirm the functional importance of miR-561 and its target DAX-1 in response to APAP exposure, we first examined the effect of miR-561 mimic or inhibitor transfection on APAP-induced HNF4α upregulation and DAX-1 downregulation in primary human hepatocytes, in which primary human hepatocytes, both HNF4α and DAX-1, were readily detected as clear single bands, with a size of ~54 and ~60 kDa, respectively (Fig. 5A). Previous studies by other groups have shown that *DAX-1* at mRNA and protein levels is clearly detected in HepG2 cells and primary human hepatocytes and mouse liver (Nedumaran et al., 2009, 2010; Laurenzana et al., 2012). However, there is another published study in which DAX-1 protein and mRNA were not detected in human liver samples

(Nakamura et al., 2009). The reasons for such a remarkable distinction may be the use of different antibodies and primers and the rapid degradation of DAX-1 protein and mRNA.

As shown in Fig. 5, A and C, treatment of primary human hepatocytes with 5 mM APAP for 24 hours increased the expression level of HNF4α by 104.7% ($P < 0.001$ by one-way ANOVA) but reduced DAX-1 protein expression level by 33.4% compared with control cells ($P < 0.001$ by one-way ANOVA), which is consistent with the result observed in HepG2 cells. Transfection of the miR-561 mimic into the primary human hepatocytes enhanced the upregulation of HNF4α by 29.9% ($P < 0.001$ by one-way ANOVA) and the downregulation of DAX-1 by 57.9% ($P < 0.001$ by one-way ANOVA; Fig. 5, A and C) compared with the control cells. As expected, transfection of the miR-561 inhibitor into primary human hepatocytes significantly reversed the increased expression of HNF4α and decreased the expression of DAX-1 caused by APAP treatment compared with cells treated with APAP only ($P < 0.01$ or 0.001 by one-way ANOVA; Fig. 5, A and C). The level of HNF4α was decreased by 41.5% ($P < 0.01$) in APAP-treated primary human hepatocytes transfected with the miR-561 inhibitor, but the level of DAX-1 was increased by 37.9% ($P < 0.001$ by one-way ANOVA; Fig. 5, A and C) by miR-561 inhibitor transfection compared with the cells treated with APAP alone. All these findings in primary human hepatocytes are consistent with those observed with HepG2 cells, verifying that miR-561 modulates APAP-induced HNF4α upregulation and DAX-1 downregulation in human hepatocytes.

To further determine the functional role of DAX-1 in NR activation upon APAP exposure, we performed experiments to examine the effect of siRNA of *DAX-1* on DAX-1 and HNF4α expression in primary human hepatocytes. Consistent with the results observed in HepG2 cells, treatment of primary human hepatocytes with 5 mM APAP for 24 hours increased HNF4α expression by 252.9% ($P < 0.001$) but decreased the expression of DAX-1 by 31.8% ($P < 0.001$ by one-way ANOVA; Fig. 5, A and C). When primary human hepatocytes were transfected with siRNA of the *DAX-1* gene, the expression level of HNF4α increased by 50.7% ($P < 0.05$ by one-way ANOVA), and the expression of DAX-1 was almost abolished (91.8% suppressed, $P < 0.001$ by one-way ANOVA; Fig. 5, A and C). In contrast, the APAP-induced DAX-1 downregulation was enhanced by DAX-1 siRNA treatment by 91.3% ($P < 0.001$ by one-way ANOVA; Fig. 5, A and C). As shown in Fig. 5, A and C, transfection of siRNA of *DAX-1* enhanced APAP-mediated upregulation of HNF4α level by 69.2% in primary human hepatocytes ($P < 0.001$ by one-way ANOVA). Taken together, these results provide additional evidence that miR-561 and its target DAX-1 are involved in APAP-induced NR activation in primary human hepatocytes.

miR-561 Regulates the Recruitment of HNF4α and its Coregulators DAX-1 and PGC1α to the *PXR* Promoter in HepG2 Cells. It is well known that HNF4α can bind to the promoter region of *PXR* and thus transactivate the expression of its target genes such as *CYP3A4* (see Supplemental Fig. 3) (Nedumaran et al., 2009). Therefore, our next question was whether HNF4α forms a complex with its coregulators that can bind to the promoter region of *PXR*. To address this question, we performed the ChIP assay in HepG2 cells transfected with miR-561 mimic with or without APAP treatment using specific antibodies against HNF4α, DAX-1, or PGC1α followed by RT-PCR analysis in HepG2 cells. Two methods were commonly used to normalize the ChIP data in this study: the Percent Input Method and the Fold Enrichment Method (Wells and Farnham, 2002). With the Percent Input Method, signals obtained from the ChIP are divided by signals obtained from an input sample. This input sample represents the amount of chromatin used in the ChIP. With the Fold Enrichment Method, the ChIP signals are divided by the no-antibody (mock IgG) signals, representing the ChIP signal as the fold increase in signal relative to the background signal. The assumption of this method is that the level of background signal is reproducible between different primer sets, samples, and replicate experiments. However, background signal levels do vary between primer sets, samples, and experiments. So we also attempted to analyze and express the ChIP data as relative to input because this includes normalization for both background levels and input chromatin going into the ChIP.

First, we compared the effect of transfection of the miR-561 mimic or inhibitor on the binding and recruitment of HNF4α, DAX-1, and PGC1α to the *PXR* promoter in HepG2 cells. When the chromatin from HepG2 cells transfected with the miR-561 mimic or inhibitor with or without APAP exposure was treated with the negative control nonspecific IgG, no enriched signal was observed that indicated the recruitment of HNF4α, DAX-1, or PGC1α onto the promoter region of *PXR* (Fig. 6).

Treatment of HepG2 cells with 5 mM APAP for 24 hours increased the recruitment of HNF4α and PGC1α to the *PXR* promoter by 92.5% and 303.2% ($P < 0.001$ by one-way ANOVA), respectively, whereas the recruitment of DAX-1 was decreased by 44.0% compared with control cells ($P < 0.05$ by one-way ANOVA; Fig. 6). The basal and APAP-induced recruitment of HNF4α to the *PXR* promoter was augmented by 80.4% and 40.5%, respectively, in HepG2 cells subject to miR-561 mimic transfection compared with control cells ($P < 0.001$ by one-way ANOVA; Fig. 6). In contrast, the basal and APAP-induced recruitment of HNF4α onto the *PXR* promoter was decreased by 52.2% and 38.2%, respectively, in HepG2 cells subject to miR-561 inhibitor transfection compared with the control cells ($P < 0.01$ by one-way ANOVA; Fig. 6).

The basal and APAP-induced recruitment of DAX-1 onto the HNF4α-binding region of the *PXR* promoter was decreased by 63.4% and 54.2%, respectively, in HepG2 cells transfected with the miR-561 mimic ($P < 0.05$ or 0.01 by one-way ANOVA; Fig. 6). In contrast, transfection of the miR-561 inhibitor into HepG2 cells enhanced the basal and APAP-induced occupancy of DAX-1 onto the HNF4α-binding region of the *PXR* promoter by 111.9% and 68.7%, respectively, compared with control cells ($P < 0.05$ or 0.01 by one-way ANOVA; Fig. 6).

We found that the basal and APAP-induced recruitment of PGC1α onto the HNF4α-binding region of the *PXR* promoter was increased by 153.9% and 99.7%, respectively, in HepG2 cells transfected with the miR-561 mimic compared with control cells ($P < 0.01$ by one-way ANOVA; Fig. 6). In contrast, transfection of the miR-561 inhibitor into HepG2 cells reduced the basal and APAP-induced occupancy of PGC1α onto the HNF4α-binding region of the *PXR* promoter by 64.8% and 46.2%, respectively, compared with control cells ($P < 0.05$ by one-way ANOVA; Fig. 6).

These data demonstrate that the basal and APAP-induced binding/recruitment of HNF4α and PGC1α onto the *PXR* promoter region is significantly augmented by miR-561 mimic transfection. However, transfection of the miR-561 mimic into HepG2 cells reduces the basal and APAP-induced recruitment and binding of DAX-1 onto the *PXR* promoter region. Transfection of the miR-561 inhibitor into HepG2 cells largely reverses these effects. Taken together, these results suggest that miR-561 regulates the binding of HNF4α and its coregulators DAX-1 and PGC1α onto the *PXR* promoter in HepG2 cells, determining the extent of transactivation of its target genes, including *PXR* and *CAR*. These data clearly indicate that miR-561 plays a role in the recruitment of HNF4α and its coregulators DAX-1 and PGC1α onto the binding region of the *PXR* promoter in HepG2 cells. miR-561 reduces the recruitment of DAX-1 and thus allows the

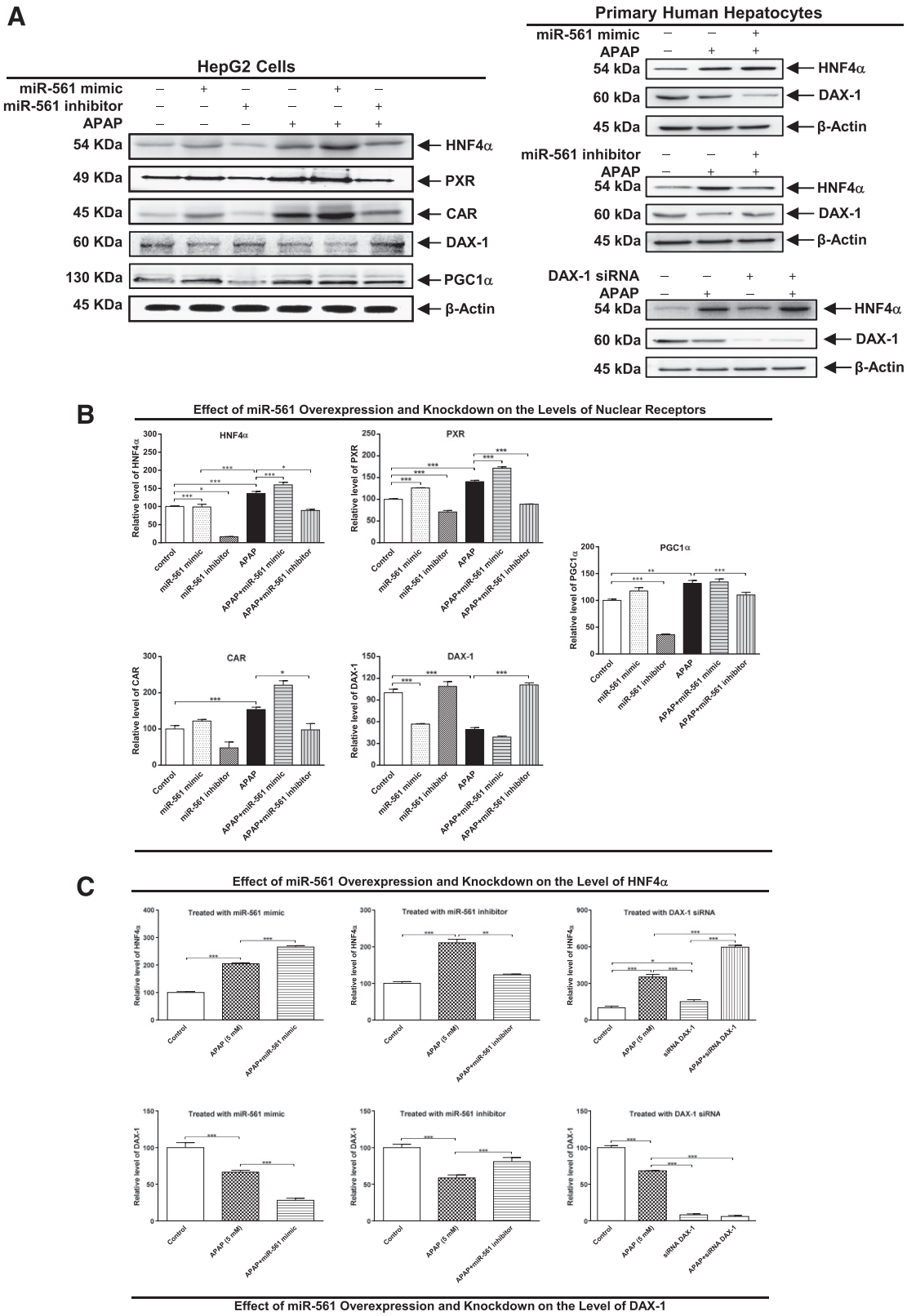

Fig. 5. Effect of overexpression or knockdown of miR-561 on the expression of HNF4α, PXR, CAR, DAX-1, and PGC1α in HepG2 cells and human primary hepatocytes. The cells were transfected with nontargeting control, miR-561 mimic, or miR-561 inhibitor for 48 hours. APAP at 5 mM was added and incubated for 24 hours after transfection. To knockdown *DAX-1*, siRNA against *DAX-1* mRNA was added to cultured primary human hepatocytes. Total cell lysates were separated on 10% SDS-PAGE, transferred to a PVDF membrane, and immunoblotted with the specific antibody against HNF4α, PXR, CAR, DAX-1, or PGC1α. (A) Representative blots of the nuclear receptors detected in HepG2 cells treated with the miR-561 mimic or inhibitor. (B) Bar graphs showing the relative blot intensity of various nuclear receptors in HepG2 cells transfected with the miR-561 mimic or inhibitor. (C) Representative blots of the HNF4α and DAX-1 detected in primary human hepatocytes treated with the miR-561 mimic, miR-561 inhibitor, or *DAX-1* siRNA. (D) Bar graphs showing the relative protein levels of HNF4α and DAX-1 in primary human hepatocytes transfected with the miR-561

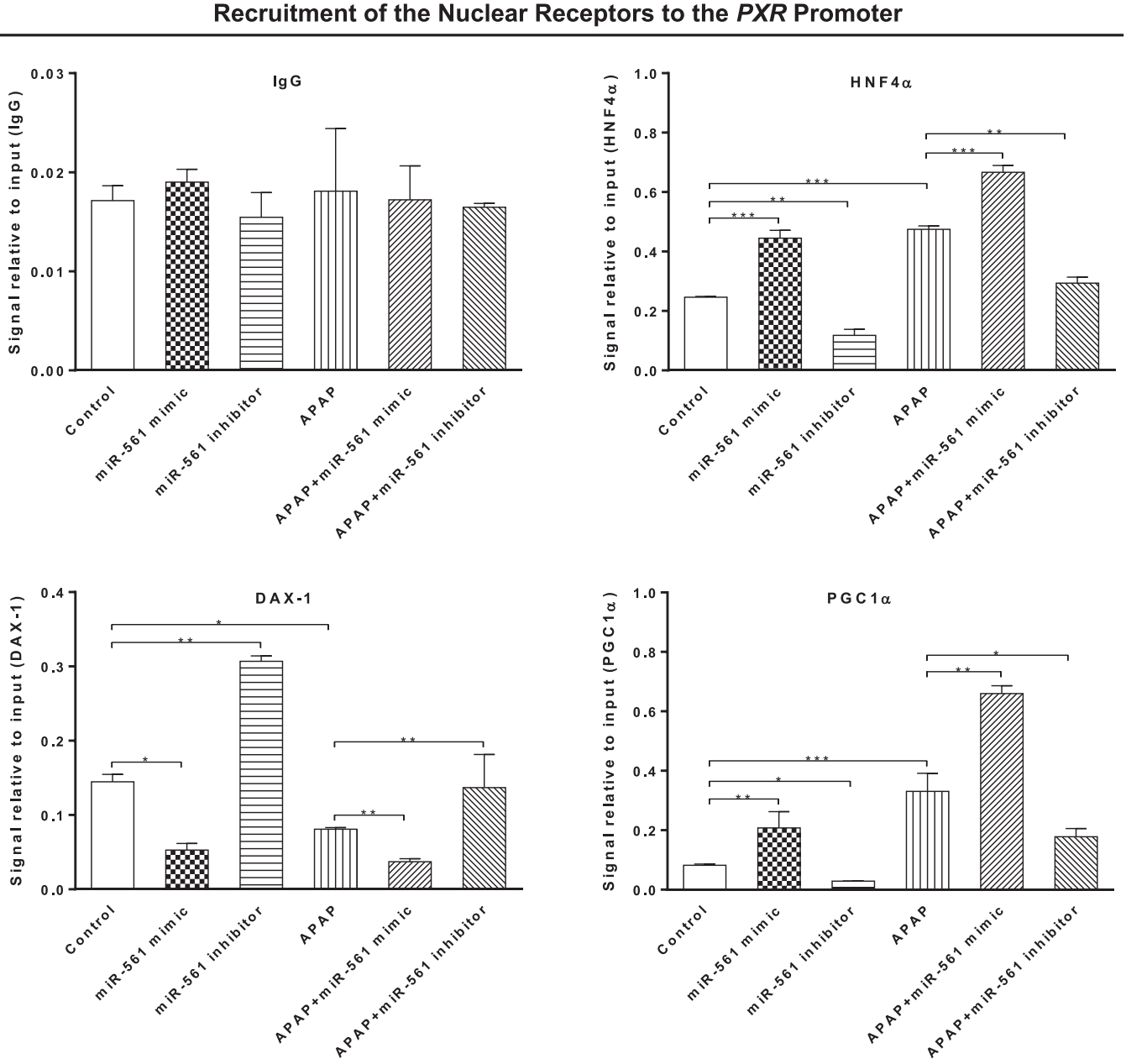

Fig. 6. miR-561 regulates the binding of HNF4α, DAX-1, and PGC1α to the *PXR* promoter in HepG2 cells. ChIP assay was performed using 4% *para*-formaldehyde-fixed samples after transfection with the miR-561 mimic or inhibitor with or without treatment of APAP at 5 mM. After immunoprecipitation using the antibodies against HNF4α, DAX-1, or PGC1α, ChIP-enriched DNA was prepared and analyzed for the recruitment of HNF4α, DAX-1, or PGC1α to the *PXR* promoter by real-time PCR. Each bar represents the mean ± S.D. obtained from three independent experiments. IgG was used as the negative control. $^*P < 0.05$; $^{**}P < 0.01$; $^{***}P < 0.001$, by one-way ANOVA and Tukey's post hoc test to compare the enrichment extent with the control cells.

formation of a more open chromatin structure that is occupied by other NRs or their coactivators.

Second, we further checked the effect of specific antibodies against HNF4α, DAX-1, or PGC1α in comparison with the nonspecific IgG on the protein-DNA complex isolated from HepG2 cells transfected with the miR-561 mimic or inhibitor with or without APAP treatment. The results are shown in Supplemental Fig. 9. Under basal conditions (i.e., without exposure to APAP), there was some recruitment of PGC1α, DAX-1, and HNF4α onto the promoter of *PXR*; antibodies specific to PGC1α, DAX-1, or HNF4α significantly enriched for the

mimic, miR-561 inhibitor, or *DAX-1* siRNA. The results are from at least three independent experiments. β-Actin served as the internal control. $^*P < 0.05$; $^{**}P < 0.01$; $^{***}P < 0.001$; by one-way ANOVA and Tukey's post hoc test to compare HNF4α, PXR, CAR, DAX-1, and PGC1α levels in treated cells with the control cells.

endogenous HNF4α binding sites in *PXR* promoter, with 4.8-, 8.4- to 14.4-fold higher inputs over that of the IgG control, respectively (see Supplemental Fig. 9). This finding reflects the need for the cells to retain basal expression of drug metabolizing enzymes and transporters that can protect the cells. When HepG2 cells were transfected with the miR-561 mimic without APAP treatment, the binding enrichment for PGC1α, DAX-1, and HNF4α was 11.0-, 2.8- and 23.4-fold higher than the IgG control (Supplemental Fig. 9). This finding indicates an increased recruitment of HNF4α and PGC1α and a decreased recruitment of DAX-1 to the *PXR* promoter when miR-561 was seen as a stress stimulus by hepatocytes. In contrast, when HepG2 cells were transfected with the miR-561 inhibitor without APAP treatment, the binding enrichment for PGC1α, DAX-1, or HNF4α was 1.9-, 19.8-, and 7.6-fold, respectively, compared with the IgG control (Supplemental Fig. 9). This finding indicates a decreased recruitment of HNF4α and PGC1α and an increased recruitment of DAX-1 to the *PXR* promoter when there was a lesser miR-561 level in hepatocytes.

When HepG2 cells were treated with APAP, the effects of transfection with the miR-561 mimic or inhibitor on the recruitment of PGC1α, DAX-1, and HNF4α onto the *PXR* promoter are shown in Supplemental Fig. 9. As expected, treatment of HepG2 cells with 5 mM APAP significantly increased the recruitment of PGC1α and HNF4α onto the *PXR* promoter, whereas binding of the corepressor DAX-1 was significantly reduced. The binding enrichment for PGC1α, DAX-1, and HNF4α was 18.3-, 4.5- and 26.3-fold higher than the IgG control (see Supplemental Fig. 9). These effects are comparable to those elicited by transfection with the miR-561 mimic. When HepG2 cells were transfected with the miR-561 mimic followed by APAP treatment, an additive effect was observed with the recruitment of PGC1α, DAX-1, and HNF4α onto the *PXR* promoter. The binding enrichment for PGC1α, DAX-1, and HNF4α was 38.3-, 2.2-, and 38.7-fold higher than the IgG control (see Supplemental Fig. 9), indicating a further increased recruitment of HNF4α and PGC1α and further reduced recruitment of DAX-1 onto the *PXR* promoter. The reason for this finding may be increased gene expression of *HNF4α* and *PGC1α* and reduced gene expression of *DAX-1*. In contrast, an antagonistic effect was observed when HepG2 cells were transfected with the miR-561 inhibitor followed by APAP treatment. The binding enrichment for PGC1α, DAX-1, and HNF4α was 10.8-, 8.3-, and 17.8-fold higher than the IgG control (see Supplemental Fig. 9), indicating a decreased recruitment of HNF4α and PGC1α and increased recruitment of DAX-1 onto the *PXR* promoter, meaning that knockdown of miR-561 passes a "safe" messenger to hepatocytes that will reduce transactivation of key nuclear receptors.

These results confirm that both HNF4α and PGC1α occupy the HNF4α-responsive region of the *PXR* promoter in HepG2 cells and that APAP treatment or transfection with the miR-561 mimic enriches their level of binding, likely via increasing gene expression of HNF4α and PGC1α. On the other hand, DAX-1 serves as a corepressor for the binding of HNF4α and PGC1α onto the *PXR* promoter in HepG2 cells; APAP treatment or transfection of the miR-561 mimic significantly reduces its recruitment to the *PXR* promoter when miR-561 inhibitor transfection results in opposing effects.

Discussion

In the present study, our bioinformatics study predicted that miR-561 could regulate a large number of targets, including DAX-1, some nuclear receptors, and other proteins that participate in the regulation of cell proliferation and apoptosis, metabolism, signaling transduction, and transport. On the other hand, DAX-1 was predicted to be probably regulated by a panel of miRNAs, including miR-561. In the following validation studies using HepG2 cells and human primary hepatocytes, we identified miR-561 as a novel target or regulator of DAX-1 that modulated APAP-caused hepatotoxicity through nuclear receptor regulation.

In HepG2 cells, we found that 1) APAP treatment induced PXR, CAR, HNF4α, and PGCα1 when miR-561 was induced but down-regulated DAX-1, the corepressor of HNF4α; 2) APAP treatment suppressed the mRNA of *DAX-1* but induced *PGC1α* mRNA, but it did not alter the expression of *HNF4*, *PXR*, and *CAR* α mRNAs; 3) APAP treatment significantly decreased DAX-1-3′-UTR reporter activity; 4) HNF4α directly interacted with DAX-1; 5) miR-561 overexpression enhanced APAP-induced activation of HNF4α, PXR, and CAR but suppressed DAX-1 expression; 6) overexpression of miR-561 significantly inhibited DAX-1-3′-UTR reporter activity; 7) miR-561 altered the binding of HNF4α, DAX-1, and PGC1α to the *PXR* promoter; 8) overexpression of miR-561 promoted APAP-induced increase of LDH release, ROS generation, and GSH depletion; and 9) inhibition of miR-561 reversed these effects. Consistently, miR-561 was found to regulate its target DAX-1 that could regulate HNF4α and consequently modulated APAP-induced hepatotoxicty in primary human hepatocytes. Taken together, our findings indicate that DAX-1 is a target of miR-561 and that it regulates HNF4α and modulates APAP-induced hepatotoxicity; miR-561 plays an important role in APAP-induced liver injury through DAX-1-mediated modulation of NR transactivation (Fig. 7, A and B). miR-561 may represent a novel therapeutic target that can be used to manage APAP overdose poisoning.

To date, more than 2000 miRNAs have been identified in humans. These RNAs are expressed in a cell- and tissue-specific manner. It is estimated that miRNAs account for ~1% of predicted genes in higher eukaryotic genomes and that up to 30% of genes within the human genome might be regulated by miRNAs. A line of evidence indicates that miRNAs have important roles in the regulation of a number of genes that participate in development, cell proliferation and apoptosis, and carcinogenesis (Xiao and Rajewsky, 2009). Many interesting findings related to differential expression of miRNA in various human diseases, including various cancers, neurodegenerative diseases, and metabolic diseases, have been reported. Increasing numbers of studies in rodents and patients suggest that many miRNAs are involved in APAP-induced liver injury (Ding et al., 2012; Jetten et al., 2012; Ward et al., 2012). The plasma levels of miR-122, miR-192, and miR-218 are significantly increased in the plasma of patients with APAP poisoning (Starkey Lewis et al., 2011, 2012). However, it is unknown how these miRNAs have a role in the pathogenesis of APAP-induced liver injuries. Our present study supports the concept that miRNAs have a critical role in APAP-induced liver injury through regulations of their target genes that contribute to APAP poisoning. Further study is needed to identify more specific hepatic miRNAs and their functions involved in process of APAP-induced liver injury. It is important that the causal role of miR-561 in APAP-induced liver injury be further investigated. Whether the modulation of miR-561 expression using miR-561 inhibitor could ameliorate APAP-induced liver injury in mice is currently under investigation in our laboratory.

The precise mechanism by which APAP upregulates miR-561 in HepG2 cells remains to be investigated. Our data suggest that oxidative stress generated by APAP treatment may be, at least in part, responsible for the ability of APAP to induce miR-561 in HepG2 cells. APAP is metabolized primarily by UGTs and SULTs, but with increasing dose of APAP, these two metabolizing pathways will be saturated and a larger portion of APAP will be switched to oxidation by microsomal CYPs. Oxidation of APAP by CYP3A4 and other CYPs will generate ROSs, such as hydrogen peroxide and superoxide,

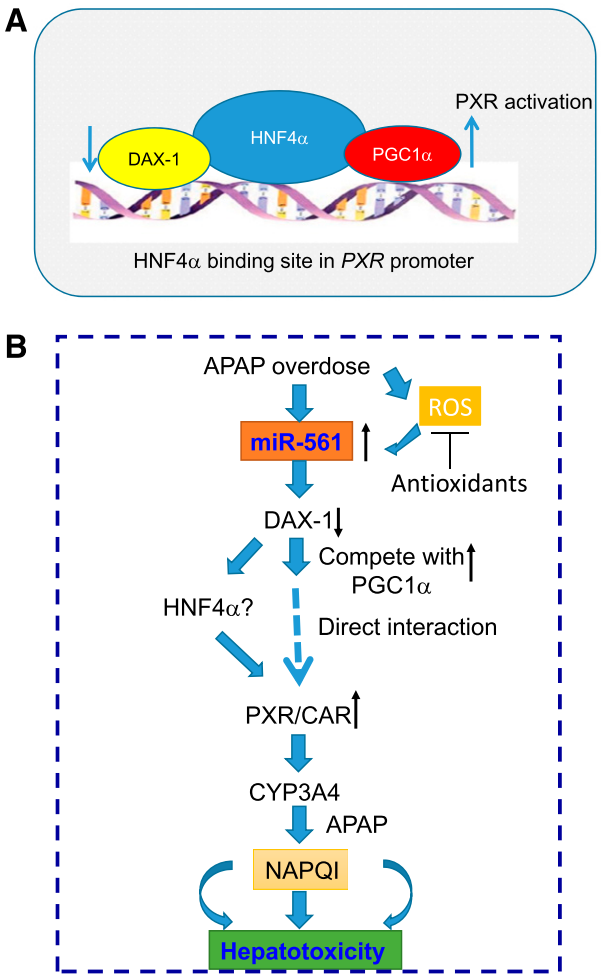

Fig. 7. Schemes to illustrate how APAP overdose causes liver injury through the activation of nuclear receptors by miR-561. (A) HNF4α-mediated regulation of its hepatic target genes is activated by elevation of cellular activity of its coactivator PGC1α, and overexpression of the HNF4α corepressor DAX-1 decreases HNF4α-mediated target gene expression. (B) Increased miR-561 levels by APAP can exaggerate APAP-induced liver injury through repressing DAX-1 expression and consequently upregulating PXR and CAR, therefor activating CYP3A4 that will convert APAP to chemically reactive and toxic metabolite NAPQI. NAPQI will covalently bind to functionally important hepatic proteins, disrupting the function and metabolism of hepatocytes, causing apoptosis, necrosis, ROS production, cytokine release, and inflammation, finally leading to liver damage that may kill the patient.

in the liver. In human liver, CYP3A4 is the most abundant and active cytochrome involved in the formation of NAPQI by overdose of APAP (Laine et al., 2009). Treatment with CYP3A4 inducers increased APAP-induced hepatotoxicity, whereas inhibitors of CYP3A4 abrogated the hepatotoxicity caused by APAP overdose (Cheng et al., 2009). Moreover, in vitro and in vivo studies suggest that antioxidant compounds can elicit beneficial effects on APAP-induced hepatotoxicity (Han et al., 2013). Therefore, it is speculated that miR-561 may be induced by ROS in APAP-induced liver injury, which can be reversed partially by antioxidants.

The miRNAs belong to a class of post-transcriptional regulators that bind to complementary sequences in the 3′-UTR of its target mRNAs, usually resulting in downregulation of specific mRNAs and inhibiting protein expression (Lewis et al., 2005; Xiao and Rajewsky, 2009). We demonstrated that the corepressor of HNF4α, DAX-1, is a target of miR-561 in response to APAP exposure in both HepG2 cells and primary human hepatocytes (Fig. 5). Our study demonstrated that miR-561 can regulate HNF4α via DAX-1-mediated pathways. The precise mechanism involved in miR-561-mediated regulation of HNF4α is unclear, but we speculate that miR-561 may directly bind to the complementary site of 3′-UTR of *HNF4α* mRNA and thus affect its expression.

DAX-1 is the member of a group of atypical nuclear receptors that lack the classic DNA-binding domain contained in other nuclear receptors, and its N-terminal region contains three short LXXL/ML motifs typically found in NR coactivators (McCabe, 2007). The C terminus of DAX1 contains a transcriptional silencing domain and an activation factor-2 domain. Its C-terminal region contains a structure characteristic of a ligand-binding domain. DAX-1 in humans is encoded by the *DAX-1* gene that is mapped to Xp21.3 (see Supplemental Fig. 2). Although it is expressed primarily in several hormone-producing tissues, including adrenal glands, pituitary gland, and hypothalamus, there is increasing evidence showing the presence of DAX-1 in human and animal livers (Ehrlund and Treuter, 2012). Our study found that there is remarkable expression of DAX-1 and its mRNA in both HepG2 cells and primary human hepatocytes (Figs. 1, 2, and 5). In general, DAX-1 serves as negative regulator of transcriptional activity of many nuclear receptors, such as HNF4α, LXRα, FXR, nerve growth factor-inducible gene B (Nur77), estrogen receptor, thyroid receptor, steroidogenic factor 1, androgen receptor, glucocorticoid receptor, liver receptor homolog-1, and peroxisome proliferator-activated receptor-γ (Nedumaran et al., 2009; Ehrlund and Treuter, 2012; Laurenzana et al., 2012). Mutations of *DAX-1* result in both X-linked congenital adrenal hypoplasia and hypogonadotropic hypogonadism. In the liver, DAX-1 could downregulate gluconeogenic genes by inhibiting HNF4α and the lipogenesis genes by inhibiting LXRα (Nedumaran et al., 2009, 2010). Our present study demonstrated that APAP upregulates miR-561 in human hepatocytes, which downregulates DAX-1 expression and its recruitment to the promoter of *PXR*, leading to the transactivation of HNF4α and PGC1α and increased recruitment of both proteins to the promoter of *PXR*, which will cause subsequent transactivation of *PXR*, ultimately inducing the expression of its target genes such as *CYP3A4* that can convert APAP to toxic NAPQI, leading to covalent binding to hepatic proteins, accumulation of ROS and proinflammatory cytokines, and eventually liver injury (Fig. 7B).

Our present study using cellular models provided enough evidence that DAX-1 is needed for miR-561-mediated regulation of HNF4α. Further studies are needed to examine how DAX-1 binds to the promoter region of *HNF4α* and the structural requirements. Animal studies are also warranted to confirm the role of DAX-1 in miR-561-mediated regulation of HNF4α.

Another novel finding of the present study is that miR-561 regulates the binding of HNF4α and its coregulators, including its coactivator PGC1α and corepressor DAX-1 to the *PXR* promoter region in HepG2 cells. It is surprising that binding of PGC1α to the *PXR* promoter was also regulated by miR-561 in HepG2 cells. Accumulating evidence suggests that DAX-1 is able to compete with coactivators of nuclear receptors for repressing their transcriptional activity. For instance, DAX-1 competes with the coactivator of LXRα, p160/steroid receptor coactivator (Nedumaran et al., 2009, 2010), the coactivator of glucocorticoid receptor and glucocorticoid receptor-interacting protein 1 (Kim et al., 2008), and the coactivator of peroxisome proliferator-activated receptor-γ, PGC1γ. Our present data show that the recruitment of DAX-1 on the *PXR* promoter is inversely correlated with the recruitment of PGC1α and HNF4α upon APAP treatment in HepG2 cells. So, although more validation studies are needed, it is logical to speculate that upregulated PGC1α binding and recruitment to the *PXR* promoter are due to decreased DAX-1 binding to the *PXR* promoter region.

HNF4α is an important transcriptional factor that regulates the expression of genes involved in xenobiotic and glucose metabolism (Kamiyama et al., 2007). Hepatic *HNF4α* expression is controlled by a complex network of proteins that bind to its promoter region (Hatzis and Talianidis, 2001). Mutations in this gene have been associated with monogenic autosomal dominant non–insulin-dependent diabetes mellitus type 1. HNF4α has been found to be essential for morphologic and functional differentiation of hepatocytes, accumulation of hepatic glycogen stores, and generation of a hepatic epithelium (Watt et al., 2003). The ectopic expression of HNF4α in fibroblasts induces a mesenchymal-to-epithelial transition, suggesting that this protein is a key regulator of the epithelial phenotype and thus plays an important role in maintaining normal liver architecture and the organization of the sinusoidal endothelium. Since we have observed that mi-561 can downregulate the expression of HNF4α, which is also significantly expressed in β-cells, we consider that mi-561 can also regulate glucose metabolism.

In this study, we identified a particular miRNA, miR-561, as a target that can regulate APAP-induced hepatotoxicity. Our bioinformatics study suggests an association between miR-561 and DAX-1, but not HNF4α. However, miR-561 may regulate HNF4α through indirect mechanisms. We have demonstrated that APAP-mediated induction of miR-561 results in DAX-1 inhibition and subsequent activation of HNF4α, which will ultimately cause PXR- or CAR-mediated CYP3A4 activation. Accumulating evidence from benchmarking studies indicates that miR-561 plays an important role in the regulation of some important genes and may affect the pathogenesis of several diseases. For example, miR-561 can downregulate 11β-hydroxysteroid dehydrogenase type 1, which converts glucocorticoid receptor–inert cortisone to receptor-active cortisol (Han et al., 2013). This important target of mi-561 was predicted in our bioinfiormatics study by both TargetScan and miRDB algorithms (see Supplemental Tables 3 and 4). It appears that miR-561 participates in the regulation of glucocorticoid metabolism and signaling and associated diseases. The tumor tissue levels of miR-561 and miR-519c-3p can accurately predict the clinical response in rectal cancer patients receiving neoadjuvant chemoradiation therapy (Ward et al., 2012). miR-561, miR-93, miR-1231, miR-524-3p, and miR-886-3p were found to be downregulated in human colon cancer stem cells (SW1116csc) (Yu et al., 2011). Overexpression of miR-93 significantly inhibited cell proliferation and colony formation of SW1116csc, and it can be expected that miR-561 overexpression can also inhibit colon cancer stem cell growth. In addition, miR-561 can regulate the engulfment adaptor PTB domain containing 1 gene in multiple myeloma (Ronchetti et al., 2008). The protein encoded by this gene is an adapter protein necessary for the engulfment of apoptotic cells by phagocytes. Further studies are needed to reveal the biologic role of miR-561 in the regulation of its important target genes, prediction of cancer therapy outcomes, and development of associated diseases.

In summary, our bioinformatics study suggests an association between miR-561 and DAX-1, but not HNF4α. We further identified miR-561 as a specific target of APAP-induced cytotoxicity in HepG2 cells and human primary hepatocytes. Our study demonstrated that APAP induces suppression of miR-561-mediated DAX-1 expression and induces the transactivation of HNF4α, and subsequent transactivation of PXR/CAR, which should ultimately cause CYP3A4/5 activation that converts APAP to toxic NAPQI and contributes to APAP-induced liver injury. Our current study shed light on the role of miRNAs in APAP-induced liver injury. Overall, this study suggests that hepatic miR-561 suppression by pharmacological or nutritional modulation might be a promising therapeutic target for the prevention and treatment of APAP-induced liver injury. Further studies are ongoing at our laboratory to examine the role of other miRNAs in APAP-induced hepatic toxicity.

Acknowledgments

The authors thank Dr. Ai-Ming Yu, Department of Biochemistry and Molecular Medicine, UC Davis School of Medicine, Sacramento, California, for valuable comments on the manuscript.

Authorship Contributions

Participated in research design: Li, Zhang, S. F. Zhou.

Conducted experiments: Li, Z. W. Zhou.

Performed data analysis: Li, He, Z. W. Zhou, T. Yang, Zhang, S. F. Zhou.

Wrote or contributed to the writing of the manuscript: Li, Y. Yang, He, Z. W. Zhou, T. Yang, Guo, Zhang, S. F. Zhou.

References

Bartel DP (2009) MicroRNAs: target recognition and regulatory functions. *Cell* **136**:215–233.
Betel D, Wilson M, Gabow A, Marks DS, and Sander C (2008) The microRNA.org resource: targets and expression. *Nucleic Acids Res* **36** (Database Issue):D149–D153.
Chai X, Zeng S, and Xie W (2013) Nuclear receptors PXR and CAR: implications for drug metabolism regulation, pharmacogenomics and beyond. *Expert Opin Drug Metab Toxicol* **9**: 253–266.
Cheng J, Ma X, Krausz KW, Idle JR, and Gonzalez FJ (2009) Rifampicin-activated human pregnane X receptor and CYP3A4 induction enhance acetaminophen-induced toxicity. *Drug Metab Dispos* **37**:1611–1621.
Ding X, Ding J, Ning J, Yi F, Chen J, Zhao D, Zheng J, Liang Z, Hu Z, and Du Q (2012) Circulating microRNA-122 as a potential biomarker for liver injury. *Mol Med Rep* **5**: 1428–1432.
Ehrlund A and Treuter E (2012) Ligand-independent actions of the orphan receptors/corepressors DAX-1 and SHP in metabolism, reproduction and disease. *J Steroid Biochem Mol Biol* **130**: 169–179.
Fannin RD, Russo M, O'Connell TM, Gerrish K, Winnike JH, Macdonald J, Newton J, Malik S, Sieber SO, and Parker J, et al. (2010) Acetaminophen dosing of humans results in blood transcriptome and metabolome changes consistent with impaired oxidative phosphorylation. *Hepatology* **51**:227–236.
Garcia DM, Baek D, Shin C, Bell GW, Grimson A, and Bartel DP (2011) Weak seed-pairing stability and high target-site abundance decrease the proficiency of lsy-6 and other microRNAs. *Nat Struct Mol Biol* **18**:1139–1146.
Han Y, Staab-Weijnitz CA, Xiong G, and Maser E (2013) Identification of microRNAs as a potential novel regulatory mechanism in HSD11B1 expression. *J Steroid Biochem Mol Biol* **133**:129–139.
Hatzis P and Talianidis I (2001) Regulatory mechanisms controlling human hepatocyte nuclear factor 4α gene expression. *Mol Cell Biol* **21**:7320–7330.
Hinson JA, Roberts DW, and James LP (2010) Mechanisms of acetaminophen-induced liver necrosis, in *Handbook Experimental Pharmacology* (Rosenthal W ed), pp. 369–405, Springer, Philadelphia.
Jakobsson T, Treuter E, Gustafsson JA, and Steffensen KR (2012) Liver X receptor biology and pharmacology: new pathways, challenges and opportunities. *Trends Pharmacol Sci* **33**: 394–404.
Jetten MJ, Gaj S, Ruiz-Aracama A, de Kok TM, van Delft JH, Lommen A, van Someren EP, Jennen DG, Claessen SM, and Peijnenburg AA,, et al. (2012) 'Omics analysis of low dose acetaminophen intake demonstrates novel response pathways in humans. *Toxicol Appl Pharmacol* **259**:320–328.
Jonker JW, Liddle C, and Downes M (2012) FXR and PXR: potential therapeutic targets in cholestasis. *J Steroid Biochem Mol Biol* **130**:147–158.
Kamiyama Y, Matsubara T, Yoshinari K, Nagata K, Kamimura H, and Yamazoe Y (2007) Role of human hepatocyte nuclear factor 4α in the expression of drug-metabolizing enzymes and transporters in human hepatocytes assessed by use of small interfering RNA. *Drug Metab Pharmacokinet* **22**:287–298.
Kim GS, Lee GY, Nedumaran B, Park YY, Kim KT, Park SC, Lee YC, Kim JB, and Choi HS (2008) The orphan nuclear receptor DAX-1 acts as a novel transcriptional corepressor of PPARgamma. *Biochem Biophys Res Commun* **370**:264–268.
Kostrubsky SE, Sinclair JF, Strom SC, Wood S, Urda E, Stolz DB, Wen YH, Kulkarni S, and Mutlib A (2005) Phenobarbital and phenytoin increased acetaminophen hepatotoxicity due to inhibition of UDP-glucuronosyltransferases in cultured human hepatocytes. *Toxicol Sci* **87**: 146–155.
Laine JE, Auriola S, Pasanen M, and Juvonen RO (2009) Acetaminophen bioactivation by human cytochrome P450 enzymes and animal microsomes. *Xenobiotica* **39**:11–21.
Laurenzana EM, Chen T, Kannuswamy M, Sell BE, Strom SC, Li Y, and Omiecinski CJ (2012) The orphan nuclear receptor DAX-1 functions as a potent corepressor of the constitutive androstane receptor (NR1I3). *Mol Pharmacol* **82**:918–928.
Lee FY, de Aguiar Vallim TQ, Chong HK, Zhang Y, Liu Y, Jones SA, Osborne TF, and Edwards PA (2010) Activation of the farnesoid X receptor provides protection against acetaminophen-induced hepatic toxicity. *Mol Endocrinol* **24**:1626–1636.
Lewis BP, Burge CB, and Bartel DP (2005) Conserved seed pairing, often flanked by adenosines, indicates that thousands of human genes are microRNA targets. *Cell* **120**:15–20.
Li J, Lu Y, Liu R, Xiong X, Zhang Z, Zhang X, Ning G, and Li X (2011) DAX1 suppresses FXR transactivity as a novel co-repressor. *Biochem Biophys Res Commun* **412**:660–666.
McCabe ER (2007) DAX1: increasing complexity in the roles of this novel nuclear receptor. *Mol Cell Endocrinol* **265-266**:179–182.
Nakamura Y, Vargas Morris C, Sasano H, and Rainey WE (2009) DAX-1A (NR0B1A) expression levels are extremely low compared to DAX-1 (NR0B1) in human steroidogenic tissues. *Horm Metab Res* **41**:30–34.

Nedumaran B, Hong S, Xie YB, Kim YH, Seo WY, Lee MW, Lee CH, Koo SH, and Choi HS (2009) DAX-1 acts as a novel corepressor of orphan nuclear receptor HNF4α and negatively regulates gluconeogenic enzyme gene expression. *J Biol Chem* **284**:27511–27523.

Nedumaran B, Kim GS, Hong S, Yoon YS, Kim YH, Lee CH, Lee YC, Koo SH, and Choi HS (2010) Orphan nuclear receptor DAX-1 acts as a novel corepressor of liver X receptor α and inhibits hepatic lipogenesis. *J Biol Chem* **285**:9221–9232.

Ronchetti D, Lionetti M, Mosca L, Agnelli L, Andronache A, Fabris S, Deliliers GL, and Neri A (2008) An integrative genomic approach reveals coordinated expression of intronic miR-335, miR-342, and miR-561 with deregulated host genes in multiple myeloma. *BMC Med Genomics* **1**:37.

Saini SP, Zhang B, Niu Y, Jiang M, Gao J, Zhai Y, Hoon Lee J, Uppal H, Tian H, and Tortorici MA, et al. (2011) Activation of liver X receptor increases acetaminophen clearance and prevents its toxicity in mice. *Hepatology* **54**:2208–2217.

Saito C, Zwingmann C, and Jaeschke H (2010) Novel mechanisms of protection against acetaminophen hepatotoxicity in mice by glutathione and *N*-acetylcysteine. *Hepatology* **51**:246–254.

Starkey Lewis PJ, Dear J, Platt V, Simpson KJ, Craig DG, Antoine DJ, French NS, Dhaun N, Webb DJ, and Costello EM, et al. (2011) Circulating microRNAs as potential markers of human drug-induced liver injury. *Hepatology* **54**:1767–1776.

Starkey Lewis PJ, Merz M, Couttet P, Grenet O, Dear J, Antoine DJ, Goldring C, Park BK, and Moggs JG (2012) Serum microRNA biomarkers for drug-induced liver injury. *Clin Pharmacol Ther* **92**:291–293.

Tirona RG, Lee W, Leake BF, Lan LB, Cline CB, Lamba V, Parviz F, Duncan SA, Inoue Y, and Gonzalez FJ, et al. (2003) The orphan nuclear receptor HNF4α determines PXR- and CAR-mediated xenobiotic induction of CYP3A4. *Nat Med* **9**:220–224.

Tujios S and Fontana RJ (2011) Mechanisms of drug-induced liver injury: from bedside to bench. *Nat Rev Gastroenterol Hepatol* **8**:202–211.

Wang K, Shindoh H, Inoue T, and Horii I (2002) Advantages of in vitro cytotoxicity testing by using primary rat hepatocytes in comparison with established cell lines. *J Toxicol Sci* **27**: 229–237.

Wang X (2008) miRDB: a microRNA target prediction and functional annotation database with a wiki interface. *RNA* **14**:1012–1017.

Ward J, Bala S, Petrasek J, and Szabo G (2012) Plasma microRNA profiles distinguish lethal injury in acetaminophen toxicity: a research study. *World J Gastroenterol* **18**:2798–2804.

Watt AJ, Garrison WD, and Duncan SA (2003) HNF4: a central regulator of hepatocyte differentiation and function. *Hepatology* **37**:1249–1253.

Wells J and Farnham PJ (2002) Characterizing transcription factor binding sites using formaldehyde crosslinking and immunoprecipitation. *Methods* **26**:48–56.

Xiao C and Rajewsky K (2009) MicroRNA control in the immune system: basic principles. *Cell* **136**:26–36.

Yu XF, Zou J, Bao ZJ, and Dong J (2011) miR-93 suppresses proliferation and colony formation of human colon cancer stem cells. *World J Gastroenterol* **17**:4711–4717.

Zhao L and Pickering G (2011) Paracetamol metabolism and related genetic differences. *Drug Metab Rev* **43**:41–52.

Address correspondence to: Dr. Shu-Feng Zhou, Associate Vice President of Global Medical Development, Department of Pharmaceutical Sciences, College of Pharmacy, University of South Florida, 12901 Bruce B. Downs Blvd., MDC 30, Tampa, FL 33612. E-mail: szhou@health.usf.edu